5466 *Biochemistry* **2009,** *48,* 5466–5482
DOI: 10.1021/bi900374c

BIOCHEMISTRY
including biophysical chemistry & molecular biology
Article

Binding Kinetics of Glucose and Allosteric Activators to Human Glucokinase Reveal Multiple Conformational States

Mathias Antoine, Jean A. Boutin,* and Gilles Ferry

Division de Pharmacologie Moléculaire et Cellulaire, Institut de Recherches Servier, 125 Chemin de Ronde, 78290 Croissy-sur-Seine, France,

Received March 5, 2009; Revised Manuscript Received April 28, 2009

ABSTRACT: Slow conformational changes have been proposed to be responsible for the kinetic positive cooperativity of glucokinase (GK) with glucose. Induced-fit and preexisting equilibrium kinetic models have been previously suggested. In the present study, equilibrium and pre-steady-state fluorescence spectroscopy has been used to resolve those conflicting reports. Multiphasic transients were observed after rapid mixing of apo-GK with glucose. Progress curve analysis revealed inconsistencies with the induced-fit model. The glucose dependence of the major kinetic phase supported the preexistence of at least two slowly interconverting GK conformers. In the absence of glucose, ≈80% of the GK population is likely poised in a largely open conformation ($K_D \approx 30$ mM). The remaining 20% is in a more compact conformation ($K_D \approx 0.2$ mM). Transients revealed three additional phases likely reflecting intermediates on the pathway between the superopen and the closed conformer. Using an intrinsically fluorescent GK activator (GKA), it was shown that GK can bind GKA in the absence of glucose, confirming the validity of the preexisting equilibrium model. Additionally, a perturbation of the GKA binding kinetic parameters after preequilibration of closed GK with an ATP analogue suggested a local rearrangement of the allosteric site upon nucleotide binding. Our data suggest that, in the absence of any ligand, GK might be able to extensively sample the conformational space delimited by the superopen and the closed conformations. The complex GK conformational equilibrium is readily shifted upon binding of ligands such as glucose or GKAs on specific GK conformers.

Glucokinase (GK,[1] also known as hexokinase D or hexokinase IV) belongs to the hexokinase family and catalyzes the phosphorylation of glucose to glucose 6-phosphate. It is the main glucose phosphorylating enzyme expressed in pancreatic β-cells and hepatocytes of most mammals, where it plays a central role in glucose homeostasis. In β-cells, GK is a critical component of the glucose sensory mechanism controlling insulin secretion (*1*). In hepatocytes, the high control strength of GK regulates the hepatic glucose metabolism (*2*). Consequently, mutations inactivating GK cause a form of diabetes called type 2 maturity onset diabetes of the young (MODY2) (*3*, *4*). Mutations enhancing the catalytic activity of GK and lowering the threshold for glucose-stimulated insulin release cause persistent hyperinsulinemia hypoglycemia of infancy (PHHI) (*5*, *6*). The existence of such activating mutations strongly suggested that development of drugs increasing GK activity might represent a promising novel therapy for the treatment of type 2 diabetes.

To fulfill its role as a glucose sensor, GK features a mild positive cooperativity coupled to a low affinity for glucose and a lack of product inhibition. This kinetic behavior is unique among other hexokinases. GK being a monomeric enzyme, the origin of the positive cooperativity for glucose had to be kinetic in nature. Two kinetic models, the "mnemonical" (*7*) and "slow-transition" (*8*) models, were proposed to account for the positive cooperativity of rat GK. Both models share the requirement for GK to slowly equilibrate between two conformations differing in their relative affinities for glucose (for a review see ref *9*). A kinetic hysteretic behavior during the approach to equilibrium was later observed, consistent with a slow glucose-induced conformational transition (*10*). This slow conformational change was further characterized by taking advantage of the intrinsic fluorescence of GK (*11*). X-ray crystallography eventually described two structures revealing GK in a superopen conformation in the absence of glucose and a major reorientation of the small domain of GK after glucose binding, switching the enzyme in a closed conformation (*12*). Following the initial work of Lin et al. (*11*) on rat GK, two independent fluorescence stopped-flow studies were performed recently with human GK. However, two completely different mechanisms were deduced from the observed fluorescence transients. On one hand, data seemed consistent with an "induced-fit" glucose binding model (*13*), whereas on the other hand, data were in

*Address correspondence to this author. Phone: +33 1 55 72 27 48. Fax: +33 1 55 72 28 10. E-mail: jean.boutin@fr.netgrs.com.

[1]Abbreviations: GK, glucokinase; GKA, glucokinase activator; GKRP, glucokinase regulatory protein; WT, wild type; TCEP, tris(2-carboxyethyl) phosphine; G6PDH, glucose 6-phosphate dehydrogenase; SPA, surface proximity assay; ITC, isothermal titration calorimetry; DSC, differential scanning calorimetry; PFK-FBP, 6-phosphofructo-2-kinase/fructose-2,6-biphosphatase; AMP-PNP, adenosine 5′-(β,γ-imino)triphosphate; DMSO, dimethyl sulfoxide.

 Published on Web 04/28/2009

agreement with a "preexisting equilibrium" model (*14*). Since then, no clarification of the glucose binding mechanism has been attempted.

Recent drug discovery projects allowed the identification of small molecule GKAs. Most of these compounds were reported *in vitro* to increase the GK activity by enhancing the apparent glucose affinity (see ref *15* for a review). Interestingly, some of the disclosed GKAs also increased the GK catalytic rate constant. GKAs are also reported to weaken the interaction between GK and its regulatory protein (GKRP) (*16*−*18*). *In vivo* studies revealed that GKAs are able to decrease glucose levels in normal and diabetic animal models (*16*, *19*−*21*).

In this work, the kinetics of the glucose-induced GK conformational changes were reinvestigated using the stopped-flow fluorescence approach in an effort to clarify the crucial mechanism linking glucose binding and GK conformational dynamics. The same methodology combined with additional equilibrium binding studies was used to decipher the binding mechanism of two reference GKAs, belonging to the amino benzamide- and cyclopropane-based series.

EXPERIMENTAL PROCEDURES

Materials. D-(+)Glucose, HEPES, G6PDH, NADP, Na-ATP, and TCEP were obtained from Sigma. GK activators LY2121260 (2-(*S*)-cyclohexyl-1-(*R*)-(4-methanesulfonylphenyl) cyclopropanecarboxylic acid thiazol-2-ylamide) from Eli Lilly & Co. and compound A (*N*-thiazol-2-yl-2-amino-4-fluoro-5-(1-methylimidazol-2-yl)thiobenzamide) from Banyu Pharmaceutical were synthesized in-house as described (*22*, *12*) and solubilized with DMSO to a 10 mM solution.

Expression and Purification of Human GK. Human glucokinase isoform 1 (pancreatic) was cloned from residue 12 to the C-terminus in the pET28 vector. The construct also possessed an N-terminal hexahistidine tag followed by the TEV cleavage site ENLYFQG. Expression was obtained in *Escherichia coli* BL21 DE3. Purification was performed on Ni-NTA followed by ion-exchange chromatography on a Hitrap Q FF column and a gel filtration on a Superdex 200 column essentially as described in Kamata et al. (*12*). Aliquots of purified GK were stored at −80 °C. Enzyme purity was checked to be >95% by SDS−PAGE and denaturing ESI-MS. GK molecular concentration was determined spectrophotometrically using an extinction coefficient at 280 nm of 35130 M^{-1} cm^{-1}. Prior to each experiment, excess glucose and glycerol were removed by dialyzing stock GK solutions twice at 4 °C and at a 1/1000 ratio (v/v) against buffer A (50 mM HEPES/Na, 100 mM NaCl, 5 mM $MgCl_2$, 2 mM TCEP, pH 7.1).

Steady-State Kinetics. GK activity was measured by monitoring the rate of G6P formation using the G6PDH/NADP-coupled enzyme assay. Initial rate measurements were carried out at 25 °C in buffer A on a Pherastar microplate reader (BMG Labtech) by following the increase of absorbance at 340 nm due to the reduction of NADP. Assays were performed in a 384-well microplate with a final volume of 50 μL per well. To determine glucose or Mg-ATP-related kinetic parameters, either glucose concentration was varied (0−50 mM) while maintaining a saturating (4 mM) Mg-ATP concentration or Mg-ATP concentration was varied (0−4 mM) while maintaining a saturating (50 mM) glucose concentration. A lag phase observed in the early time course of the reaction was omitted for the determination of the initial rate. This lag phase is likely due to the coupled-enzyme assay, as already described (*23*). Initial rate data obtained with varying glucose concentrations were fitted to the Hill equation (eq 1).

$$k_{obs} = \frac{k_{cat} S^h}{K_{0.5}{}^h + S^h} \quad (1)$$

Initial rate data obtained with varying Mg-ATP concentrations or in the presence of GK activators were fitted to the Michaelis−Menten equation. Nonlinear least-squares regression analysis was performed with SigmaPlot 9.01.

Equilibrium Binding of Glucose to GK. Fluorescence measurements were performed at room temperature on a Varioskan Flash microplate reader (Thermo), using 96-well, half-bottom, black microplates. Glucose binding to GK induces a conformational change and an increase of the intrinsic Trp fluorescence emission intensity. Apparent glucose binding to GK was monitored by measuring the GK fluorescence emission spectra after incubation of 5 μM GK with various glucose concentrations (0−50 mM) in buffer A. Excitation was set at 280 and 295 nm to observe emission from 300 to 550 nm. Background fluorescence was subtracted, and maximum emission values were plotted as a function of glucose concentration and fitted to the hyperbolic binding equation (eq 2), where F_{obs} represents the observed fluorescence, F_{max}, the fluorescence of the GK−glucose complex, [Glc], glucose concentration, and K_{Dapp}, the apparent dissociation constant of the GK−glucose complex.

$$F_{obs} = \frac{F_{max}[Glc]}{K_{Dapp} + [Glc]} \quad (2)$$

Equilibrium Binding of Activators to GK. Fluorescence measurements were performed at room temperature on a Varioskan Flash microplate reader (Thermo), using 96-well, half-bottom, black microplates. Intrinsic fluorescence emission of compound A is strongly enhanced when bound to GK, thus providing a direct probe to assess its binding to GK. Binding of compound A and LY2121260 to GK was studied according to the general framework described by Roehrl et al. (*24*), except that the observed variable used in our study was fluorescence intensity instead of anisotropy. Direct binding of compound A to GK was carried out by incubating 0.5 μM compound A and an increasing GK concentration in buffer A supplemented with 5% DMSO. Binding was assessed in three different conditions: without glucose, with 100 mM glucose, or with 100 mM glucose complemented with 4 mM AMP-PNP. Intrinsic fluorescence of compound A was specifically measured by setting excitation at 360 nm and reading emission at 425 nm. Data were fitted to the quadratic equation (eq 3), with F_{obs} representing observed fluorescence, F_{SB}, the fraction of bound compound A, f_{AB}, fluorescence level of bound compound A, f_{AF}, fluorescence level of free compound A, K_{DCA}, dissociation constant of the GK−compound A complex, [A], total concentration of compound A, and [GK], total concentration of GK. Competitive binding between fluorescent compound A and nonfluorescent LY2121260 to GK was carried out in a similar way by incubating 0.5 μM compound A, 0.8 μM GK, and an increasing LY2121260 concentration. Data were fitted to the complete competitive binding model described by

Scheme 1

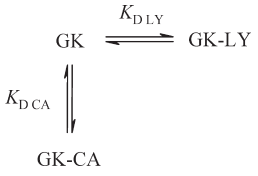

Scheme 1 and eq 4, with [LY] representing the total concentration of LY2121260 and K_{DLY} the dissociation constant of the GK−LY2121260 complex.

$$F_{obs} = F_{SB}f_{AB} + (1 - F_{SB})f_{AF}$$

with

$$F_{SB} = \frac{K_{DCA} + [A] + [GK] - \sqrt{(K_{DCA} + [A] + [GK])^2 - 4[A][GK]}}{2[A]} \quad (3)$$

$$F_{obs} = F_{SB}f_{AB} + (1 - F_{SB})f_{AF}$$

with

$$F_{SB} = \frac{2\sqrt{(d^2 - 3e)}\cos(\theta/3) - d}{3K_{DCA} + 2\sqrt{(d^2 - 3e)}\cos(\theta/3) - d}$$

$$d = K_{DCA} + K_{DLY} + [A] + [LY] - [GK]$$

$$e = ([LY] - [GK])K_{DCA} + ([A] - [GK])K_{DLY} + K_{DCA}K_{DLY}$$

$$f = -K_{DCA}K_{DLY}[GK]$$

$$\theta = \arccos\left[\frac{-2d^3 + 9de - 27f}{2\sqrt{(d^2 - 3e)^3}}\right] \quad (4)$$

Pre-Steady-State Binding Kinetics of Glucose and Activators to GK. Transient kinetics were measured at 25 °C with a SFM-300 stopped-flow mixer fitted with a FC-15 cell and coupled to a MOS-200 M rapid spectrophotometer fitted with a 150 W Xe−Hg lamp (Bio-Logic). Typical dead time was 2.6 ms. GK tryptophans were excited at 295 nm to minimize photobleaching and excitation of tyrosine, to reduce inner-filter effects arising from activators or nucleotides, and to take advantage of the strong 297 nmHg emission line. GK-bound compound A was excited at 360 nm to minimize both GK and free compound A excitation and to take advantage of the strong Hg emission line at 365 nm. Two photomultipliers were used, the first one to record GK fluorescence via a 320 nm cutoff filter combined with a UG11 band-pass filter to block compound A fluorescence and the second one to record compound A fluorescence via a 400 nm cutoff filter. Binding experiments were performed under pseudo-first-order conditions by mixing an equal volume (75 μL) of GK and ligand (glucose, AMP-PNP, or GKA) in buffer A, complemented with 5% DMSO when GKAs were present. GK concentration after mixing was 1 μM. When preequilibrated

Scheme 2: Simplified Cyclic "Preexisting Equilibrium" Model Describing GK Interaction with Glucose[a]

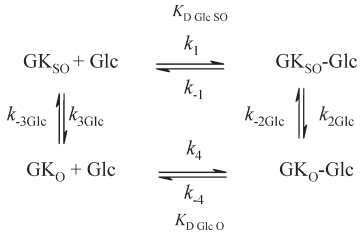

[a] GK_{SO} and GK_O are the low- and high-affinity conformers described by the glucose dependence of $k_{obs3\,Glc}$, and Glc glucose.

Scheme 3

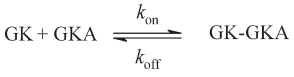

binary and ternary GK complexes were studied (GK−glucose, GK−glucose−AMP-PNP, GK−glucose−GKA), excess ligand (s) were included in both syringes, whereas the variable ligand was kept in only one syringe. At least five traces for each variable ligand concentration were recorded. To increase the signal/noise ratio, an oversampling strategy was used. Data acquisition was triggered 40 ms before the flow stop with a fast sampling rate, followed by a second time base with a slower sampling rate, averaging the data still acquired at the initial fast sampling rate. When necessary, an additional time base was included to capture early kinetic transitions occurring during the first 200 ms. Data were then reduced off-line by applying a logarithmic sampling routine included in the BioKine software provided with the instrument.

Pre-Steady-State Data Analysis. Fluorescence traces were first analyzed individually with the BioKine software as a sum of up to four exponential terms, as described by eq 5, with n being the number of exponentials, a_i, the amplitude of the ith exponential, $k_{obs\,i}$, the rate constant of the ith exponential, c, the trace end point, and bt accounting for the slow linear drift caused by photobleaching.

$$y = \sum_{i=1}^{n} a_i e^{-k_{obs\,i}t} + bt + c \quad (5)$$

When best fits required up to four exponentials, justification of the four terms was qualitatively assessed by the visual inspection of the residual plot from the regression. Additionally, a quantitative statistical model comparison between the four exponential equation and the three and two exponential equations was also carried out with Prism 4.02, using the extra sum-of-squares F-test and the corrected Akaike's Information Criteria (AICc) tools included in the software.

k_{obs} values were plotted against ligand concentration and fitted to the relevant equation. When a biphasic dependence of k_{obs} against glucose concentration was observed, data were fitted to the cyclic four-step preexisting equilibrium model described by Scheme 2 and eq 6 by nonlinear regression analysis, as described previously (*14*). When a linear dependence was observed with GKA, data were fitted to the one-step binding mechanism described by Scheme 3 and eq 7. When a biphasic dependence of k_{obs} against GKA concentration was observed, data were

Scheme 4: Simplified Cyclic "Preexisting Equilibrium" Model Describing GK Interaction with GKA[a]

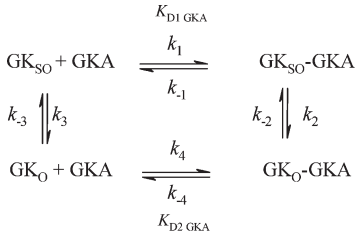

[a] GK_{SO} and GK_O are the low- and high-affinity conformers described by the GKA dependence of $k_{obs4\,GKA}$ and GKA glucokinase activator: compound A or LY2121260.

fitted to the cyclic four-step preexisting equilibrium model described by Scheme 4 and eq 8.

$$k_{obs} = \frac{k_{3\,Glc} + [Glc]\frac{k_{2\,Glc}}{K_{D\,Glc\,SO}}}{1 + \frac{[Glc]}{K_{D\,Glc\,SO}}} + \frac{k_{-3\,Glc} + [Glc]\frac{k_{-2\,Glc}}{K_{D\,Glc\,O}}}{1 + \frac{[Glc]}{K_{D\,Glc\,O}}} \quad (6)$$

$$k_{obs} = k_{on}[GKA] + k_{off} \quad (7)$$

$$k_{obs} = \frac{k_{3\,GKA} + [GKA]\frac{k_{2\,GKA}}{K_{D1\,GKA}}}{1 + \frac{[GKA]}{K_{D1\,GKA}}} + \frac{k_{-3\,GKA} + [GKA]\frac{k_{-2\,GKA}}{K_{D2\,GKA}}}{1 + \frac{[GKA]}{K_{D2\,GKA}}} \quad (8)$$

Kinetic Simulations. Demo version of Berkeley Madonna and KinTek Explorer were used for modeling and testing of different kinetic mechanisms for ligand binding to GK.

RESULTS

Steady-State Kinetics and Equilibrium Glucose Binding. The recombinant human GK used in this study is the pancreatic isoform, deleted from its 11 first residues, His-tagged on its N-terminus, and purified to homogeneity. Steady-state kinetic behavior of the His-tagged truncated GK was determined for glucose and ATP. GK showed positive cooperativity with glucose (n_H = 1.8, $K_{0.5\,Glc}$ = 8.5 mM) while hyperbolic saturation was observed with ATP ($K_{M\,ATP}$ = 0.7 mM). k_{cat} was 54 s^{-1}.

As expected (*12*, *19*), addition of 20 μM compound A or LY2121260 resulted in the loss of positive cooperativity with glucose and in activation of GK catalysis. GK activators increased both k_{cat} and the apparent glucose affinity ($k_{cat\,CA}$ = 64 s^{-1}, $K_{M\,Glc\,CA}$ = 0.76 mM, $k_{cat\,LY}$ = 75 s^{-1}, $K_{M\,Glc\,LY}$ = 0.63 mM).

As also described (*11*, *13*−*15*, *26*), glucose addition to GK induced a strong increase of the tryptophan fluorescence emission. No significant spectral shift was observed with excitation set at 295 nm. The apparent binding affinity of glucose was close to the values previously determined ($K_{Dapp\,Glc}$ = 5.5 mM, data not shown). Kinetic parameters and apparent K_D displayed by the His-tagged truncated GK are similar to the reported values for wild-type GK, confirming the functional integrity of the truncated enzyme.

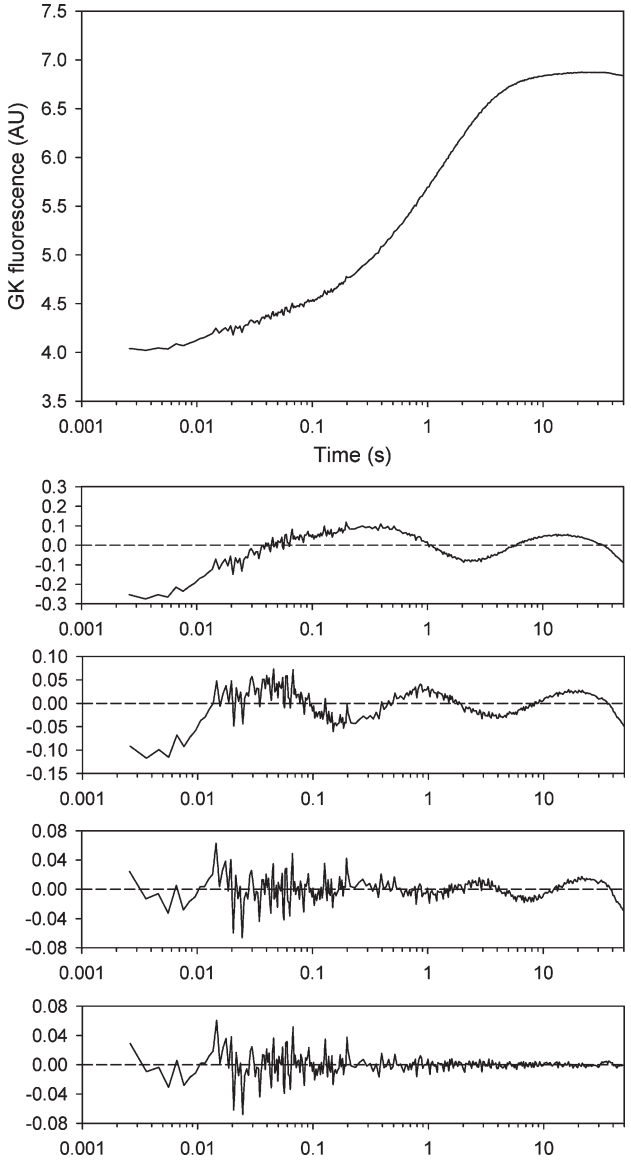

FIGURE 1: Time-resolved glucose-induced conformational change monitored by GK intrinsic fluorescence (λ_{exc} = 295 nm). Representative fluorescence transient recorded after rapid mixing of apo-GK (1 μM) and glucose (50 mM) in buffer A. The upper frame shows the recorded transient; lower frames show the residuals for the best fit to one, two, three, and four exponentials.

Pre-Steady-State Glucose Binding Kinetics. Pre-steady-state fluorescence spectroscopy has been used to investigate the kinetics of glucose binding to GK (*13*, *14*). However, discrepancies between reports remain unresolved. Previous fluorescence stopped-flow studies reported either monophasic or biphasic transients, leading to diametrically opposite mechanism (see Discussion).

In our hands, the fluorescence traces recorded after rapid mixing of apo-GK and glucose were clearly multiphasic, and the best fit was obtained with four exponential terms, as seen from the residual plots (Figure 1). Additionally, both the *F*-test and the AICc methods were used to quantitatively compare the quality of the fits between the four, three, and two exponential models. Comparing the two and three exponential fits to the four exponential fit lead to *F* ratios of 383 and 56, respectively, and thus to the statistical rejection of the two and three phase fits compared to the four phase fit. Using the AICc method, differences in AICc between the two and three exponential fits

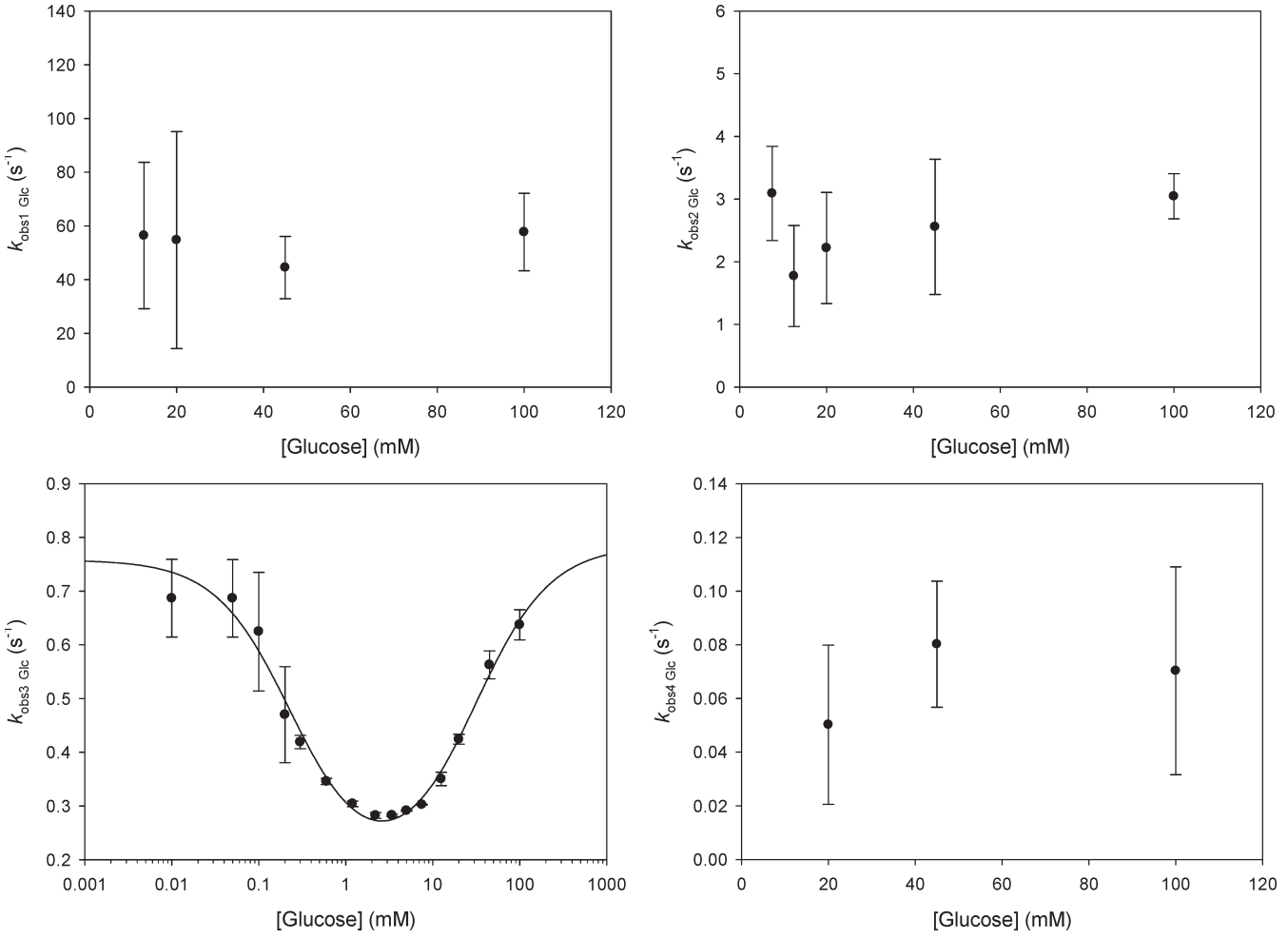

FIGURE 2: Dependence of $k_{obs1\,Glc}$, $k_{obs2\,Glc}$, $k_{obs3\,Glc}$, and $k_{obs4\,Glc}$ on glucose concentration. The solid line is a fit of $k_{obs3\,Glc}$ to eq 6 with parameters $k_{3\,Glc}$ = 0.13 s^{-1}, $k_{-3\,Glc}$ = 0.63 s^{-1}, $K_{D\,Glc\,SO}$ = 30 mM, $k_{2\,Glc}$ = 0.8 s^{-1}, $k_{-2\,Glc}$ = 0.05 s^{-1}, $K_{D\,Glc\,O}$ = 0.24 mM. Note the semilogarithmic scale for $k_{obs3\,Glc}$.

and the four exponential fit were 560 and 94, respectively, clearly indicating that the four exponential fit model is largely preferred.

Using high glucose concentration, the third phase accounted for two-thirds of the total amplitude, while the first, second, and fourth phase represented each 5−10% of the total amplitude. Thus, only the third phase was observable for the lowest glucose concentrations used. When plotted against glucose concentration, total fluorescence intensity yielded an hyperbolic trend, readily fitted to eq 2 and led to an apparent $K_{Dapp\,Glc}$ value of 4.3 mM, in agreement with the microplate equilibrium data (data not shown). Repeating the experiment on a stopped-flow instrument similar to the ones used in previous reports (SX18MV-R; Applied PhotoPhysics) led to similar results.

The observed rate constant for the third phase, $k_{obs3\,Glc}$, exhibited a biphasic dependence on the glucose concentration, as observed by Kim et al. (*14*). The $k_{obs3\,Glc}$ values decreased hyperbolically from 0.7 s^{-1} at 0.01 mM glucose to 0.3 s^{-1} between 2 and 5 mM glucose before increasing at concentrations above 5 mM and starting to level off at high glucose concentrations (above 50 mM). It is noteworthy that $k_{obs3\,Glc}$ values are very close to the k_{obs} measured by Kim et al. (*14*).

This kinetic behavior is consistent with a cyclic equilibrium involving four species: two preexisting GK conformers, both of them being able to bind glucose, and the same conformers complexed with glucose, as described by Scheme 2. For the sake of clarity, and as assumed by Kim et al. (*14*), the two GK conformers could tentatively be assigned to the superopen (GK_{SO}) and open (GK_O) conformations proposed by Kamata et al. (*12*). Assuming that glucose binding is spectroscopically silent, the decrease in $k_{obs3\,Glc}$ reflects the slow unimolecular isomerization between GK_{SO} and GK_O, followed by the rapid binding of glucose, yielding GK_O−Glc: $k_{obs3\,Glc}$ decreases from ($k_{3\,Glc}$ + $k_{-3\,Glc}$) to $k_{3\,Glc}$. This reaction path will be referred to as route A. The increase in $k_{obs3\,Glc}$ describes the rapid binding of glucose to GK_{SO} yielding GK_{SO}−Glc, followed by the slow unimolecular isomerization from GK_{SO}−Glc to GK_O−Glc: $k_{obs3\,Glc}$ increases from $k_{-2\,Glc}$ to ($k_{-2\,Glc}$ + $k_{2\,Glc}$). This reaction path will be referred to as route B. Decoupling between the two kinetic paths A and B is granted by $K_{D\,Glc\,SO}$ being greater than $K_{D\,Glc\,O}$.

The $k_{obs3\,Glc}$ values were then fitted to eq 6. Derivation of a set of six kinetic parameters from a single set of $k_{obs3\,Glc}$ values, with resulting $k_{2\,Glc}$, $k_{-2\,Glc}$, $k_{3\,Glc}$, and $k_{-3\,Glc}$ values being quite close, led to high systematic standard errors. Nevertheless, the resulting fit showed a good correlation with the experimental data, with a coefficient of determination R_2 = 0.91 (Figure 2). Based on this fit, the preequilibrium between GK_{SO} and GK_O is governed by a forward rate constant $k_{3\,Glc}$ = 0.13 s^{-1} and a reverse rate constant $k_{-3\,Glc}$ = 0.63 s^{-1}. $K_{D\,Glc\,SO}$ was 30 ± 7 mM and $K_{D\,Glc\,O}$ was 0.24 ± 0.04 mM. The equilibrium between GK_{SO}−Glc and GK_O−Glc is governed by a forward rate constant $k_{2\,Glc}$ = 0.8 s^{-1} and a reverse rate constant $k_{-2\,Glc}$ = 0.05 s^{-1}.

Assuming an irreversible GK_{SO}−Glc to GK_O−Glc transition ($k_{-2\,Glc} = 0$) led to an improvement of the fit error (fit error below 0.04 s^{-1}) but did not significantly alter the remaining parameters; neither improved the R_2 value. This assumption is however mechanistically invalid, as introduction of such an irreversible step would lead to the loss of the fluorescence glucose dependence. Based on this analysis, no conclusion could be drawn regarding the intrinsic value of $k_{-2\,Glc}$, apart from the fact that it is < 0.1 s^{-1}. It is noteworthy that no information regarding the on and off rate constants for glucose (k_{1Glc}, k_{4Glc} and k_{-1Glc}, k_{-4Glc}) could be derived from the data.

The ratio k_{-3Glc}/k_{3Glc} predicts that, in the absence of glucose, about 80% of apo-GK is in the GK_{SO} conformation. This result is key in the attribution of the increased fluorescence quantum yield to a specific species. Indeed, if the fluorescence increase is linked to glucose binding to GK, as proposed previously (*14*), and assuming reasonable k_1 and k_4 for glucose binding (1×10^7 M^{-1} s^{-1}) for both GK_{SO} and GK_O, and two k_{-1} and k_{-4} values compatible with measured $K_{D\,Glc\,SO}$ and $K_{D\,Glc\,O}$ ($k_{-1} = 3 \times 10^5$ s^{-1} for GK_{SO}−Glc and $k_{-4} = 2 \times 10^4$ s^{-1} for GK_O−Glc), simulation predicts a burst of fluorescence during the dead time of the instrument, followed by a slow exponential rise. The simulated burst amplitude increases with glucose concentration, as GK_{SO} becomes saturated by glucose. This behavior is not observed experimentally. If one now assumes that the increased fluorescence arises from the conformational transition from GK_{SO} to GK_O, regardless of the glucose binding, simulation now predicts the absence of a fluorescence burst and the observation of a slow single exponential. This analysis supports the assignation of the low quantum yield species to both GK_{SO} and GK_{SO}−Glc and the high quantum yield species to both GK_O and GK_O−Glc.

Despite a fairly high imprecision due to their low amplitudes, the observed rate constants for the three other phases, $k_{obs1\,Glc}$, $k_{obs2\,Glc}$, and $k_{obs4\,Glc}$, were essentially independent of glucose concentration, suggesting the existence of three additional unimolecular isomerizations, with on average $k_{obs1\,Glc} \approx 50$ s^{-1}, $k_{obs2\,Glc} \approx 2.5$ s^{-1}, and $k_{obs4\,Glc} \approx 0.07$ s^{-1}. Importantly, in contrast to a previous report from Heredia et al. (*13*), no linear dependence with glucose concentrations was observed for the fastest phase, $k_{obs1\,Glc}$, thus ruling out the observation of a bimolecular binding event.

Addition of three extra steps to the simplified mechanism described by Scheme 2 generates many complex mechanisms, potentially complicated by partitioning steps. Global analysis of kinetic traces integrates the variation of both observed rate constants and signal amplitudes, thus providing a better resolving power than the traditional fitting approach relying only on observed rate constant analysis. However, because of the weak amplitudes of the three apparent additional phases and the related absence of signal for glucose concentration less than 5−10 mM, combined with the increase of parameters to be fitted, global analysis of the raw fluorescence transients was not undertaken.

Fluorescence Properties of Compound A. The UV−visible absorption spectrum of compound A (Figure 3) dissolved in buffer A containing 5% DMSO featured a major peak centered at 275 nm and a minor peak centered at 345 nm. When exciting compound A at these two wavelengths, a broad fluorescence emission centered at 455 nm was recorded. Excitation spectra confirmed the two λ_{max} at 275 and 345 nm (Figure 4A). When switching to more apolar solvents like ethanol and DMSO, a red shift of the two excitation maxima, a blue shift of the emission maximum, and an increase of the quantum yield occurred (data not shown). Those results establish that compound A is an environment-sensitive fluorophore.

Equilibrium Binding of Compound A and LY2121260 to GK. Addition of an equivalent of GK in 100 mM glucose to free compound A in buffer A containing 5% DMSO led to

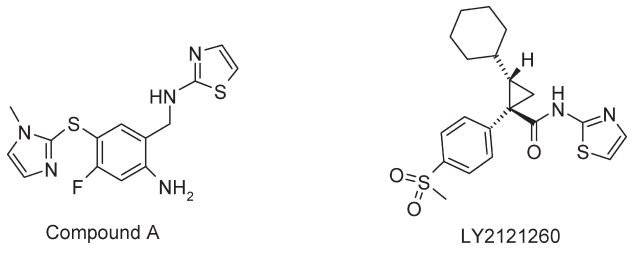

FIGURE 3: Chemical structures of compound A and LY121260.

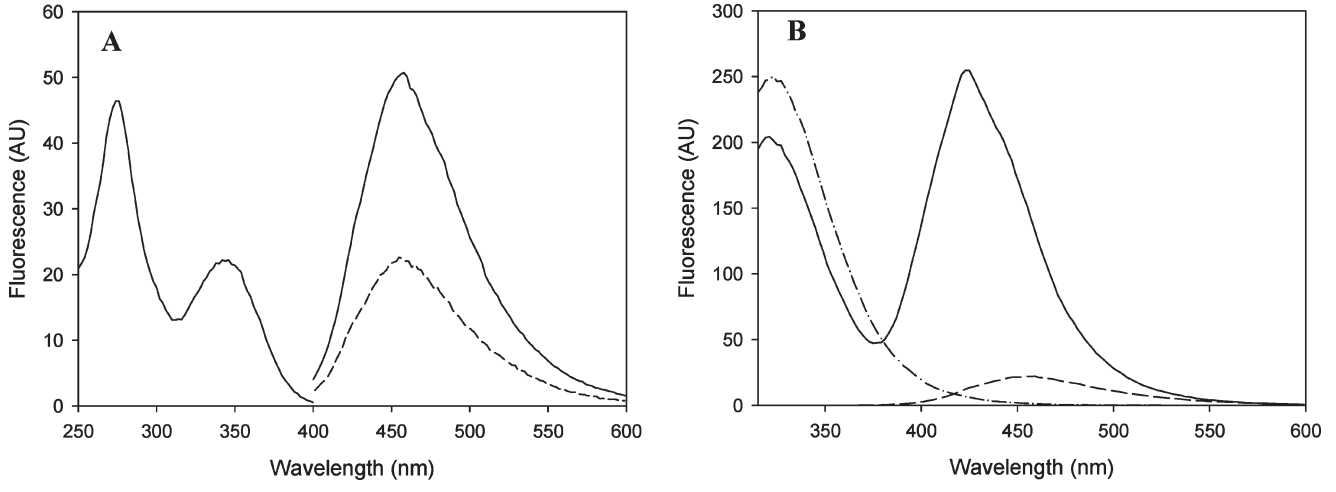

FIGURE 4: Fluorescence properties of compound A. (A) Fluorescence excitation and emission spectra of 20 μM compound A in buffer A containing 5% DMSO. The excitation spectrum was recorded from 240 to 400 nm with emission fixed at 455 nm. Emission spectra were recorded from 400 to 600 nm with excitation fixed at 275 nm (solid line) or at 345 nm (dashed line). (B) Fluorescence emission spectra of 20 μM free compound A (dashed line), 20 μM GK + 100 mM glucose (dash-dot line), and 20 μM compound A + 20 μM GK + 100 mM glucose (solid line). Excitation was set at 295 nm.

similar results than observed with apolar solvents. Compound A excitation maxima were red shifted to 280 and 360 nm (not shown), while the emission maximum was blue shifted to 425 nm, together with a strong increase of the quantum yield (Figure 4B). Thus, binding of compound A to the allosteric site of GK can conveniently and selectively be monitored through the enhancement of its intrinsic fluorescence. Additionally, a slight quenching of the GK fluorescence emission was also observed.

To determine the equilibrium dissociation constant K_{DCA} for binding of compound A to GK, the intrinsic fluorescence emission of compound A was recorded as a function of total GK concentration. Titration of compound A with GK resulted in a sigmoidal increase of compound A intrinsic fluorescence against the log of total GK concentrations. In the presence of 100 mM glucose, K_{DCA} was estimated ≈0.07 μM. In the presence of 100 mM glucose and 4 mM AMP-PNP, K_{DCA} was estimated ≈0.04 μM. In the absence of any ligands, K_{DCA} was estimated ≈9 μM (Figure 5A). It should be stressed that because of the strong sensitivity of the fit toward compound A concentration, the fitted K_D values are only provided as estimates (a 3-fold decrease of the fixed compound A concentration in the fitting procedure led to a 10-fold increase of K_{DCA}, with a reasonably good fit to the data).

Competitive binding assays were performed in the presence of compound A to determine the equilibrium dissociation K_{DLY} for binding of LY2121260 to GK. The intrinsic fluorescence emission of compound A was recorded as a function of total LY2121260 concentration. Titration of the preformed GK−compound A complex with LY2121260 resulted in a sigmoidal decrease of compound A intrinsic fluorescence relative to the log of total LY2121260 concentrations. In the presence of 100 mM glucose, K_{DLY} was estimated ≈0.4 μM; in the presence of 100 mM glucose and 4 mM AMP-PNP, K_{DLY} was estimated ≈0.3 μM (Figure 5B).

Pre-Steady-State Binding of Compound A and LY212160 to GK in the Presence of 100 mM Glucose. To better understand the interaction between GK and its activators, the kinetics of binding have been investigated by the stopped-flow fluorometry approach. Both compound A intrinsic fluorescence and GK intrinsic fluorescence were used to monitor binding of compound A to GK, whereas GK fluorescence was the only available probe to monitor binding of LY2121260 to the allosteric site.

Upon mixing of GK with compound A, in the presence of 100 mM glucose, GK fluorescence displayed a biphasic transient composed of a major fast quenching followed by a weak slow fluorescence increase (Figure 6A). The slow phase was only defined for the two highest concentrations used. Each phase could be individually fitted to a single exponential. When monitoring compound A fluorescence on the same time scale, a biphasic transient was also observed, composed of a major fast burst of fluorescence followed by a weak slow increase of the signal (Figure 6B). Each phase could be individually fitted to a single exponential.

Observed rate constants for the fast phases were linearly dependent on compound A concentration (insets in Figure 6A,B), consistent with a simple bimolecular association of GK_O and compound A, yielding a quenching of GK_O fluorescence. Linear regression of the data yielded a similar second-order association rate constant $k_{on\,CA}$ of 1.13×10^6 M^{-1} s^{-1} for both fluorescence readings and a dissociation rate constant $k_{off\,CA}$ of 0.5 s^{-1} and 3 s^{-1}, observed with GK and compound A fluorescence, respectively. To obtain a better precision on the measure of this slow dissociation rate constant, k_{off} was independently measured by the displacement of compound A from the allosteric site of GK_O by excess LY2121260, monitored by compound A fluorescence. The resulting decay in compound A fluorescence confirmed its displacement by LY2121260 (Figure 6C). The transient could be fitted to a double exponential, with the fastest one representing more than two-thirds of the total amplitude. The second rate was only 2-fold slower. While it is unclear why two phases are observed, one might suggest that it could arise from the contribution of two closed GK conformers. We assumed that the fastest k_{obs} reflected the major contribution. The k_{obs} values were independent of LY2121260 concentrations. This observation confirmed that dissociation of compound A is the rate-limiting

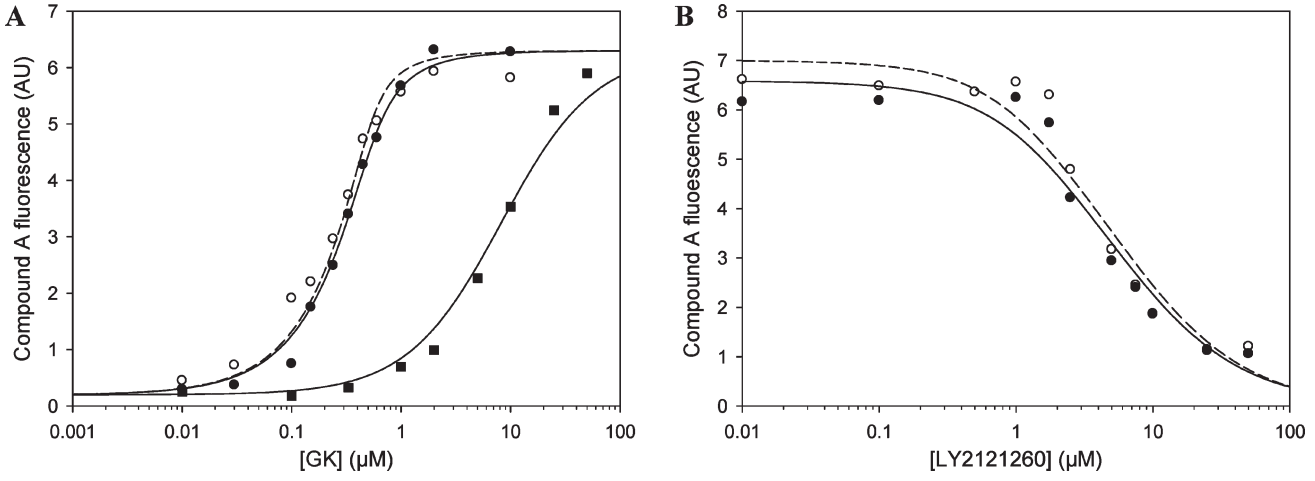

FIGURE 5: Equilibrium binding of compound A and LY2121260 to GK, monitored by compound A intrinsic fluorescence, in buffer A containing 5% DMSO. (A) Direct binding experiment between 0.5 μM compound A and GK, in the presence of 100 mM glucose and 4 mM AMP-PNP (○), in the presence of 100 mM glucose (●), or in the absence of any ligands (■). The lines are fits to eq 3, with K_{DCA} ≈0.04 μM in the presence of 100 mM Glc and 4 mM AMP-PNP (dashed line), ≈0.07 μM in the presence of 100 mM Glc (solid line), and ≈9 μM in the absence of any ligand (solid line). (B) Competitive displacement of 0.5 μM compound A from 0.8 μM GK by LY2121260, in the presence of 100 mM glucose (●) and in the presence of 100 mM glucose and 4 mM AMP-PNP (○). The lines are fits to eq 4 using K_{DCA} values measured in (A) with K_{DLY} ≈ 0.4 μM in the absence of AMP-PNP (solid line) and K_{DLY} ≈ 0.3 μM in the presence of AMP-PNP (dashed line). Experiments were performed in buffer A containing 5% DMSO.

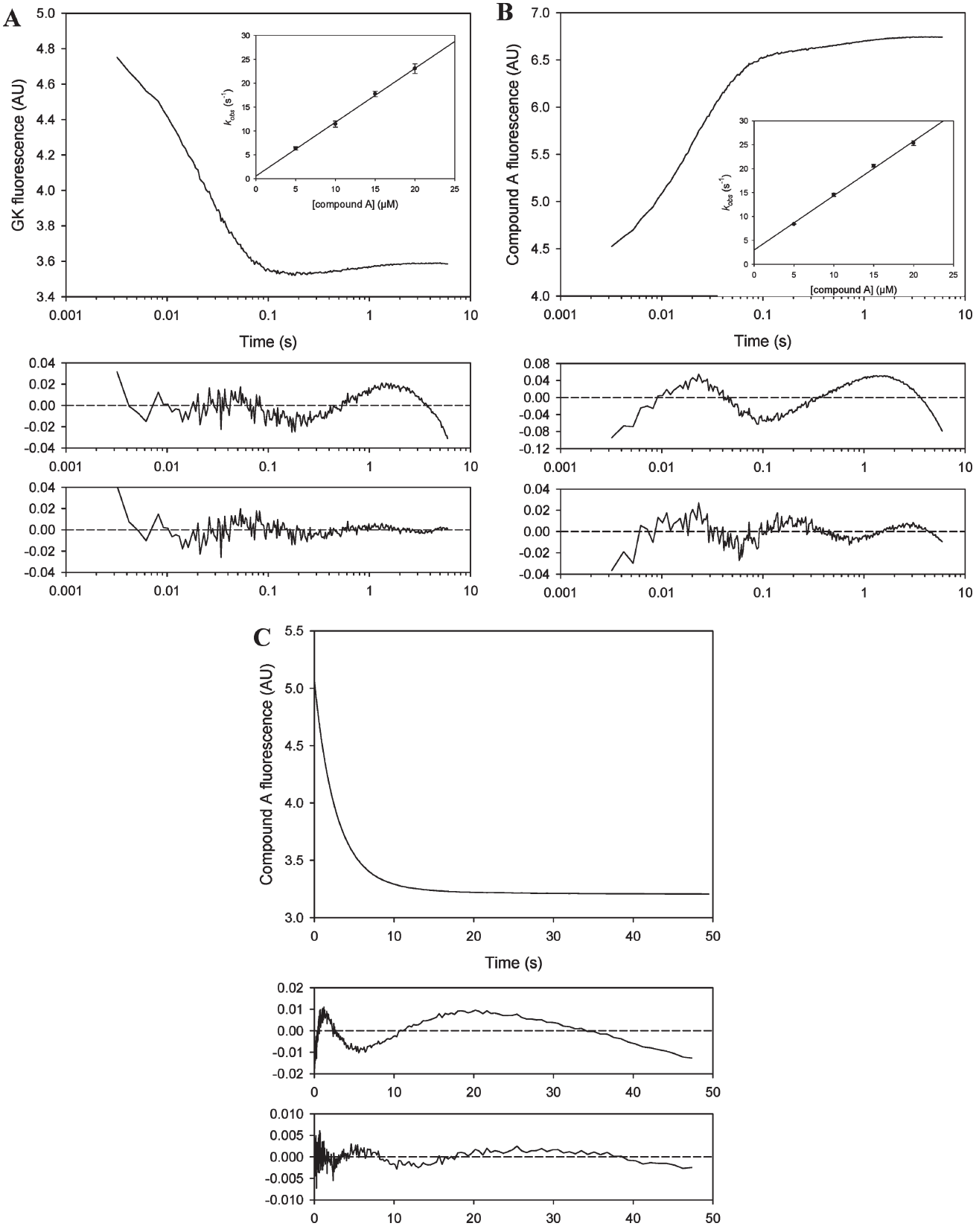

FIGURE 6: Kinetics of the interaction of compound A with the GK−glucose complex. (A) GK (1 μM) was mixed with compound A (20 μM) in the presence of 100 mM glucose in buffer A containing 5% DMSO, and the GK fluorescence was recorded (λ_{exc} = 295 nm). (B) Same as (A) but compound A fluorescence was recorded (λ_{exc} = 360 nm). Upper frames show the recorded transients; lower frames show the residuals for the best fit to one and two exponentials. Insets show the linear dependence of k_{obs} against compound A concentration. (C) Dissociation of compound A was measured by preequilibrating GK (1 μM) with compound A (10 μM) and mixing it with excess LY2121260 (50 μM) in the presence of 100 mM glucose, while monitoring compound A fluorescence (λ_{exc} = 360 nm). Upper frames show the recorded transients; lower frames show the residuals for the best fit to one and two exponentials.

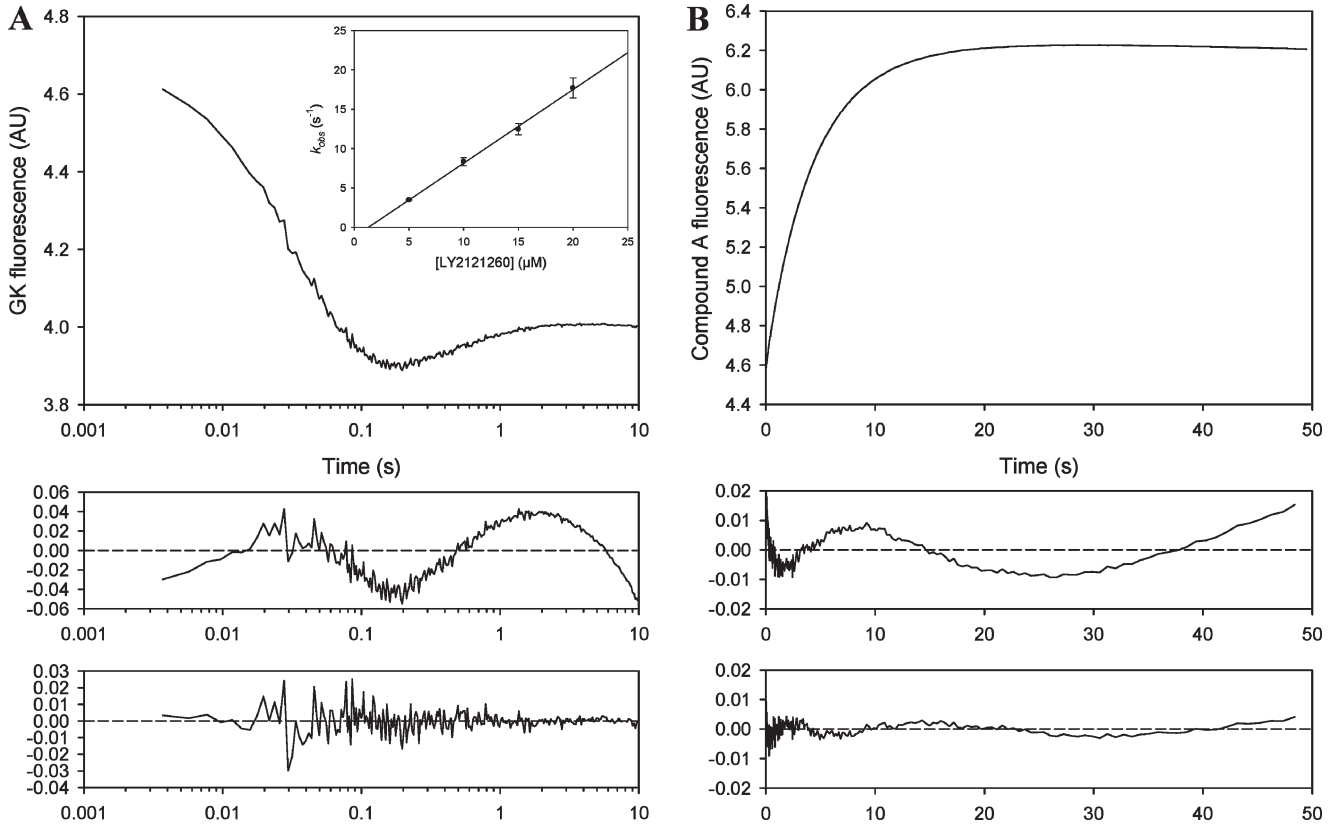

FIGURE 7: Kinetics of the interaction of LY2121260 with the GK−glucose complex. (A) GK (1 μM final) was mixed with LY2121260 (20 μM final) in the presence of 100 mM glucose in buffer A containing 5% DMSO, and the GK fluorescence was recorded (λ_{exc} = 295 nm). The upper frame shows the recorded transient; lower frames show the residuals for the best fit to one and two exponentials. The inset shows the linear dependence of k_{obs} against LY2121260 concentration. (B) Dissociation of LY2121260 was measured by preequilibrating GK (1 μM final) with LY2121260 (10 μM final) and mixing it with excess compound A (50 μM) while monitoring compound A fluorescence (λ_{exc} = 360 nm). The upper frame shows the recorded transient; lower frames show the residuals for the best fit to one and two exponentials.

step in the displacement reaction, not the LY2121260 association. Thus, $k_{obs} = k_{off\,CA} = 0.43\ s^{-1}$. $K_{D\,CA}$ calculated from $k_{on\,CA}$ and $k_{off\,CA}$ was 0.36 μM.

Observed rate constants for the slow phases following compound A binding were essentially independent of compound A concentration, with a similar k_{obs} value of 1.2 s^{-1} for both fluorescence readings. The slow phase could tentatively be assigned to an induced-fit unimolecular isomerization of the GK_O−compound A complex or to the binding of glucose to the activator-bound GK.

Binding of LY2121260 under the same conditions led to similar results. Upon mixing of GK_O with LY2121260 in the presence of 100 mM glucose, GK fluorescence displayed a biphasic transient (Figure 7A). Analysis of the fast phase led to a k_{on} value for LY2121260 slightly lower than its counterpart for compound A: $k_{on\,LY} = 0.94 \times 10^6\ M^{-1}\ s^{-1}$. Displacement of bound LY2121260 by an excess of compound A allowed for the precise determination of the dissociation rate constant: $k_{off\,LY} = 0.37\ s^{-1}$ (Figure 7B). $K_{D\,LY}$ calculated from $k_{on\,LY}$ and $k_{off\,LY}$ was 0.40 μM, in good agreement with the equilibrium data.

Observed rate constants for the slow phase following LY2121260 binding were essentially independent of LY2121260 concentration, with a k_{obs} value of 1.5 s^{-1}. The slow phase is therefore tentatively assigned to an induced-fit unimolecular isomerization of the GK−LY2121260 complex or, more likely, to the binding of glucose to the activator-bound GK.

Pre-Steady-State Binding of Compound A and LY212160 to GK in the Presence of 100 mM Glucose and 4 mM AMP-PNP. Upon mixing of $GK_{O\,AMP\text{-}PNP}$ with compound A, in the presence of 100 mM glucose and 4 mM AMP-PNP, GK fluorescence displayed a fast monophasic quenching (Figure 8A). When monitoring compound A fluorescence on the same time scale, a monophasic signal increase was observed (Figure 8B). Fast phases were fitted to a single exponential. Observed rate constants were linearly dependent on compound A concentration, consistent with a simple bimolecular association of GK_O and its activator (insets in Figure 8A,B). Linear regression of the data yielded an average second-order association rate constant $k_{on\,CA}$ of $1.67 \times 10^6\ M^{-1}\ s^{-1}$, faster than in the presence of glucose only, and a dissociation rate constant $k_{off\,CA}$ of 0 s^{-1} and 4.8 s^{-1} for GK and compound A fluorescence, respectively. Displacement of compound A from the allosteric site of GK_O by an excess of LY2121260, monitored by compound A fluorescence, resulted in a $k_{off\,CA}$ of 0.62 s^{-1} (Figure 8C). Kinetically determined $K_{D\,CA\,AMP\text{-}PNP}$ was 0.37 μM, undistinguishable from the $K_{D\,CA}$.

Binding of LY2121260 under the same conditions led to similar results. Upon mixing of GK with LY2121260 in the presence of 100 mM glucose and 4 mM PNPAMP, GK fluorescence displayed a fast monophasic transient (Figure 9A). Regression analysis led to a k_{on} value for LY2121260 slightly faster than in the presence of glucose only ($k_{on\,LY} = 1.09 \times 10^6\ M^{-1}\ s^{-1}$). Displacement of bound LY2121260 by excess compound A allowed for the precise determination of the dissociation rate constant ($k_{off\,LY} = 0.30\ s^{-1}$) (Figure 9B). $K_{D\,LY}$ calculated from $k_{on\,LY}$ and $k_{off\,LY}$ was 0.27 μM, in agreement with the equilibrium data.

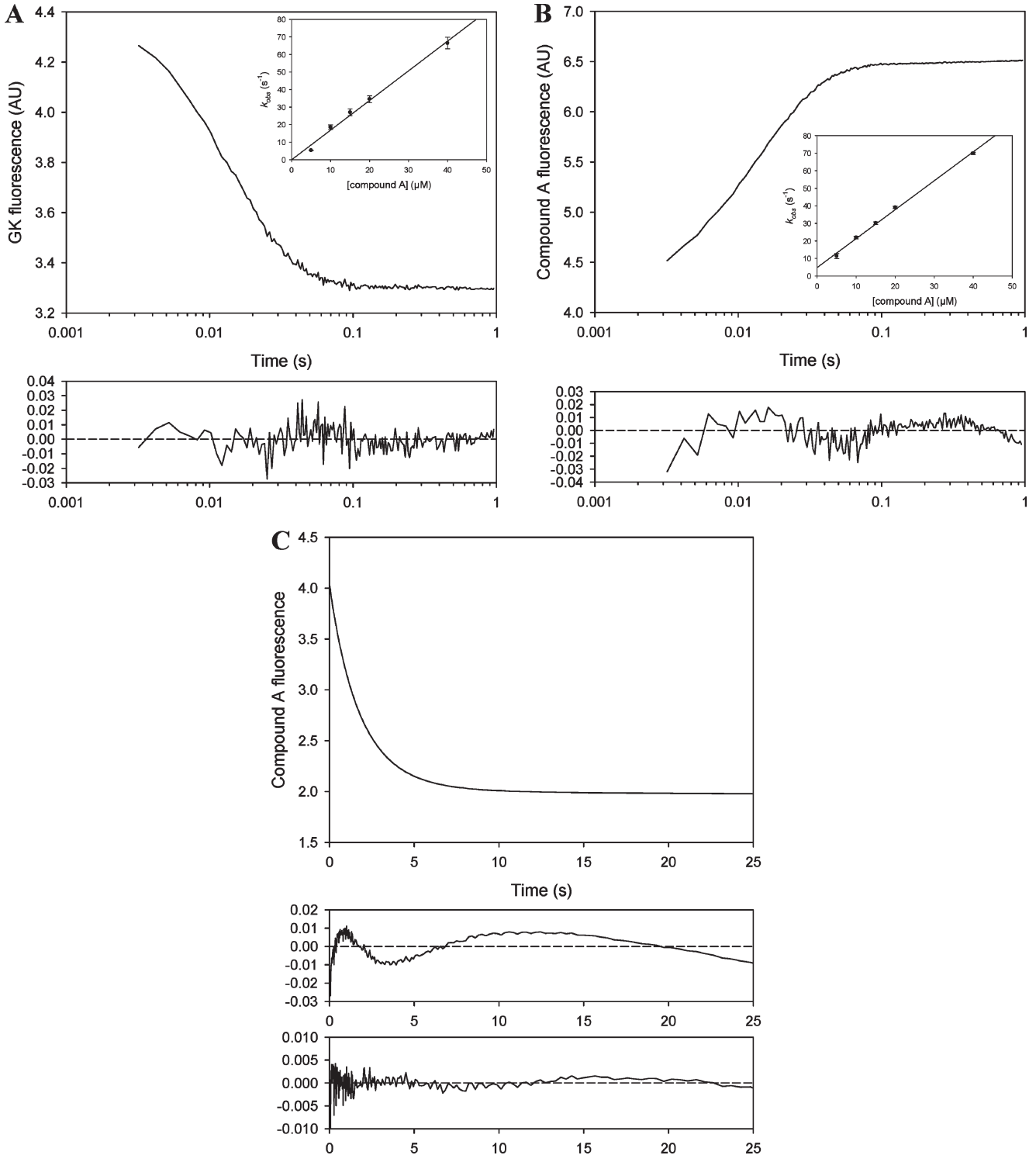

FIGURE 8: Kinetics of the interaction of compound A with the GK−glucose−AMP-PNP complex. (A) GK (1 μM final) was mixed with compound A (20 μM final) in the presence of 100 mM glucose and 4 mM AMP-PNP in buffer A containing 5% DMSO, and the GK fluorescence was recorded (λ_{exc} = 295 nm). (B) same as (A) but compound A fluorescence was recorded (λ_{exc} = 360 nm). Upper frames show the recorded transients; lower frames show the residuals for the best fit to one exponential. Insets show the linear dependence of k_{obs} against compound A concentration. (C) Dissociation of compound A was measured by preequilibrating GK (1 μM final) with compound A (10 μM final) and mixing it with excess LY2121260 (50 μM) in the presence of 100 mM glucose and 4 mM AMP-PNP while monitoring compound A fluorescence (λ_{exc} = 360 nm). The upper frame shows the recorded transient; lower frames show the residuals for the best fit to one and two exponentials.

Pre-Steady-State Binding of Compound A and LY212160 to GK in the Absence of Any Ligands. Previous structural and biochemical studies led to the conclusion that the absence of glucose precluded the binding of GK activators to the protein. However, this conclusion did not integrate the presence of 10−20% GK_O in the total apo-GK population resulting from the conformational preexisting equilibrium. The combination of the preexisting equilibrium mechanism and the structural models suggests that GKAs could bind to the minority GK_O subpopulation preexisting in the absence of glucose, hence lowering the GK_O concentration and further shifting the equilibrium from GK_{SO} toward the GK_O conformer. However, this prediction was

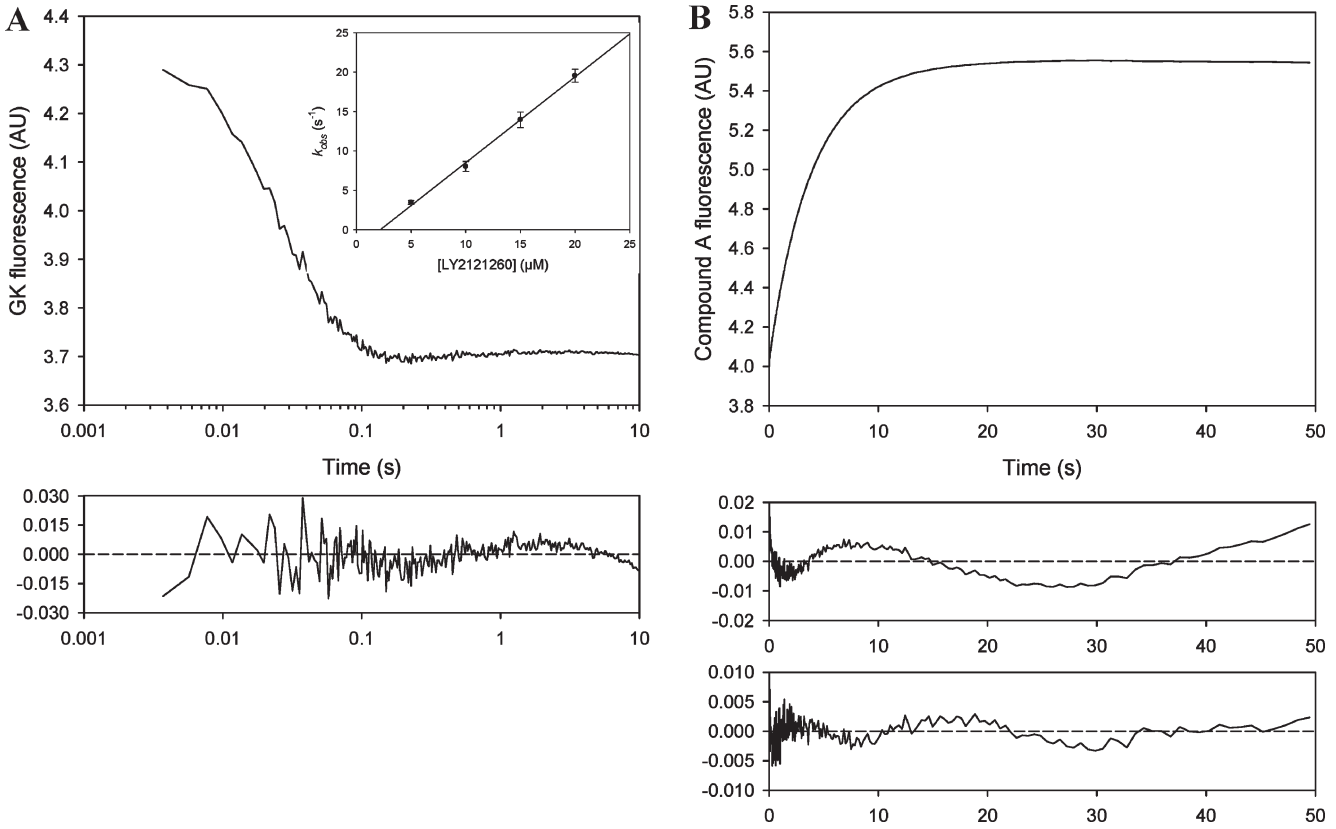

FIGURE 9: Kinetics of the interaction of LY2121260 with the GK−glucose−AMP-PNP complex. (A) GK (1 μM final) was mixed with LY2121260 (20 μM final) in the presence of 100 mM glucose and 4 mM AMP-PNP in buffer A containing 5% DMSO, and the GK fluorescence was recorded (λ_{exc} = 295 nm). The upper frame shows the recorded transient; the lower frame shows the residuals for the best fit to one exponential. The inset shows the linear dependence of k_{obs} against LY2121260 concentration. (B) Dissociation of LY2121260 was measured by preequilibrating GK (1 μM final) with LY2121260 (10 μM final) and mixing it with excess compound A (50 μM) while monitoring compound A fluorescence (λ_{exc} = 360 nm). The upper frame shows the recorded transient; lower frames show the residuals for the best fit to one and two exponentials.

not entirely supported by experimental results, as more complex results were obtained.

Indeed, upon mixing of GK with compound A, in the absence of any ligand, GK fluorescence displayed a fast but weak quenching followed by a larger slow increase (Figure 10A). The transient could be satisfactorily fitted with two exponential terms. The fast quenching could likely be assigned to the binding of compound A to the minority GK_O conformer. However, accurate determination of the associated rate constant was obscured by the weak amplitude of the signal (about 10% of the total amplitude). Thus, no quantitative analysis of the data was attempted. The slow increase of GK fluorescence was reminiscent of the transition from GK_{SO} to GK_O induced by glucose. Unexpectedly, the observed rate constant for this second phase ($k_{obs2\,CA}$) exhibited a biphasic dependence on compound A concentration. The value of $k_{obs2\,CA}$ decreased hyperbolically from 0.19 s^{-1} at 1 μM compound A to 0.1 s^{-1} between 10 and 20 μM compound A before slowly increasing at a concentration above 20 μM and starting to level off at high compound A concentration (above 60 μM) (Figure 10A). This kinetic pattern is similar to the one observed previously with glucose and suggests a kinetic mechanism based on the cyclic preexisting equilibrium model. Fitting of $k_{obs2\,CA}$ to eq 7 led to fairly high systematic errors on the parameters values. However, a good correlation was observed between the fit and the data (R_2 = 0.98) with the following parameters: $k_{3\,CA}$ = 0.06 s^{-1}, $k_{-3\,CA}$ = 2.5 s^{-1}, $K_{D2\,CA}$ = 0.06 μM, $k_{2\,CA}$ = 0.12 s^{-1}, $k_{-2\,CA}$ = 0.01 s^{-1}, and $K_{D1\,CA}$ = 45 μM (inset in Figure 10A). It should be stressed that because of the limited access to low GKA concentrations, fitting was not sensitive to the $k_{-3\,CA}$ value. Constraining the $k_{-3\,CA}$ value to 0.8 s^{-1} during the fitting procedure did not significantly change the five other parameters. Thus, the k_{-3} values determined in this study for GKA binding have to be considered solely as rough estimates.

It should be noticed that the amplitude of the GK fluorescence increase observed after rapid mixing with compound A reached saturation for concentrations >40 μM, with a fluorescence intensity representing around 30−40% of the equilibrium intensity observed with compound A and saturating glucose. Thus, in the absence of glucose, compound A might not be able to fully shift the GK_{SO}−GK_O equilibrium toward GK_O.

When monitoring compound A fluorescence on the same time scale, a multiphasic increase was observed (Figure 10B). At high compound A concentrations, the transient could be fitted with four exponential terms, as seen from the residual plots. Additionally, both the *F*-test and the AICc methods were used to quantitatively compare the quality of the fits between the four, three, and two exponentials models, as described for the glucose binding. Again, comparing the two and three exponential fits to the four exponential fit lead to *F* ratios of 220 and 41, respectively, thus to the statistical rejection of the two and three phase fits compared to the four phase fit. Using the AICc method, differences in AICc between the two and three exponential fits and the four exponential fit were 395 and 71, respectively, clearly indicating that the four exponential fit model is largely preferred.

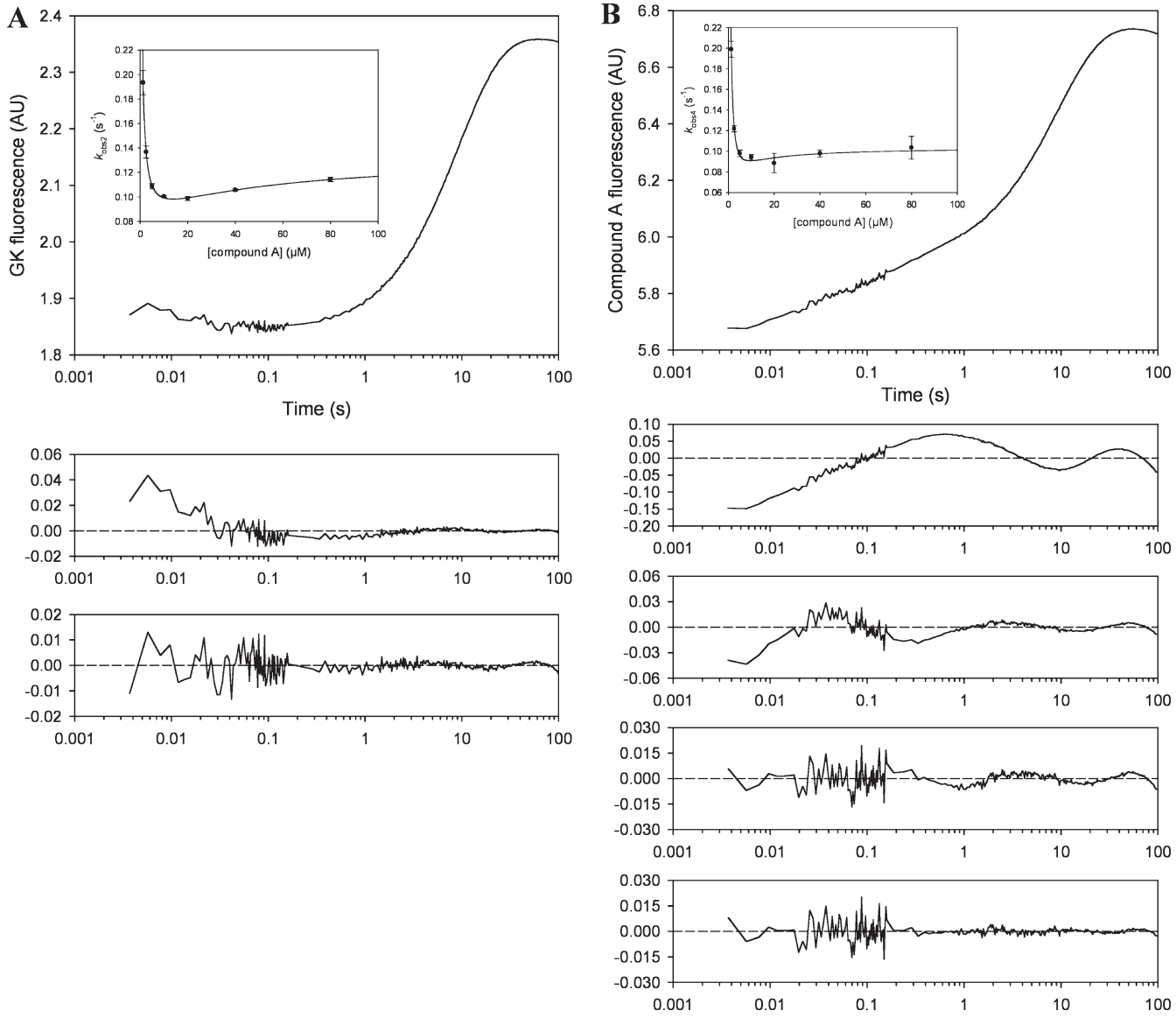

FIGURE 10: Kinetics of the interaction of compound A with apo-GK in the absence of glucose. (A) Apo-GK (1 μM) was rapidly mixed with compound A (80 μM) in buffer A containing 5% DMSO, and the GK fluorescence was recorded (λ_{exc} = 295 nm). The upper frame shows the recorded transient; lower frames show the residuals for the best fit to one and two exponentials. (B) Same as (A) but compound A fluorescence was recorded (λ_{exc} = 360 nm). The upper frame shows the recorded transient; lower frames show the residuals for the best fit to one, two, three, and four exponentials. Insets show the dependence of the major k_{obs} against compound A concentration. The solid line is a fit to eq 8 with parameters $k_{3CA} = 0.06\ s^{-1}$, $k_{-3CA} = 2.5\ s^{-1}$, $K_{D2CA} = 0.06\ \mu M$, $k_{2CA} = 0.12\ s^{-1}$, $k_{-2CA} = 0.01\ s^{-1}$, and $K_{D1CA} = 45\ \mu M$ for the GK fluorescence reading and $k_{3CA} = 0.002\ s^{-1}$, $k_{-3CA} = 8.4\ s^{-1}$, $K_{D2CA} = 0.02\ \mu M$, $k_{2CA} = 0.10\ s^{-1}$, $k_{-2CA} = 0.0001\ s^{-1}$, and $K_{D1CA} = 5\ \mu M$ for the compound A fluorescence reading.

The fourth phase accounted for more than 70% of the total amplitude. The observed rate constant for the fourth phase, k_{obs4}, exhibited a biphasic dependence on compound A concentration, as observed previously for k_{obs2} measured via GK fluorescence, with almost identical k_{obs} values. Fitting to eq 6 led to poorer errors than obtained with GK fluorescence; still, a good correlation was observed between the fit and the data (R_2 = 0.95) (inset in Figure 10B). Estimated parameters were $k_{3CA} = 0.002\ s^{-1}$, $k_{-3CA} = 8.4\ s^{-1}$, $K_{D2CA} = 0.02\ \mu M$, $k_{2CA} = 0.10\ s^{-1}$, $k_{-2CA} = 0.0001\ s^{-1}$, and $K_{D1CA} = 5\ \mu M$.

Although suffering of a significant imprecision due to their low amplitudes, the observed rate for the three other phases seemed to be essentially independent of compound A concentration, suggesting the presence of three additional unimolecular isomerizations, as observed with glucose binding to apo-GK. On average, the rate constants observed with compound A were close to their counterparts observed with glucose, with $k_{obs1CA} = 60-80\ s^{-1}$, $k_{obs2CA} = 5\ s^{-1}$, and $k_{obs3CA} = 0.3\ s^{-1}$. It is probable that the fastest k_{obs}, k_{obs1CA}, represents contributions from both compound A binding and fast GK isomerization. The inability to observe these three minority phases while monitoring GK fluorescence could result from the low amplitude of these phases and the likely combination of signals of opposite amplitude from compound A binding to GK (quenching of GK fluorescence) and GK isomerizations (increase of GK fluorescence).

Interestingly, parameters obtained from either GK or compound A fluorescence showed that the kinetic K_{D2CA} lied in the range of the equilibrium K_{DCA} for GK_O, suggesting that the minority GK_O conformation described in the glucose binding experiment is also involved in compound A binding. It is then tempting to assign GK_{SO} as the major conformer involved in the preexisting equilibrium with GK_O, also able to bind compound A as defined

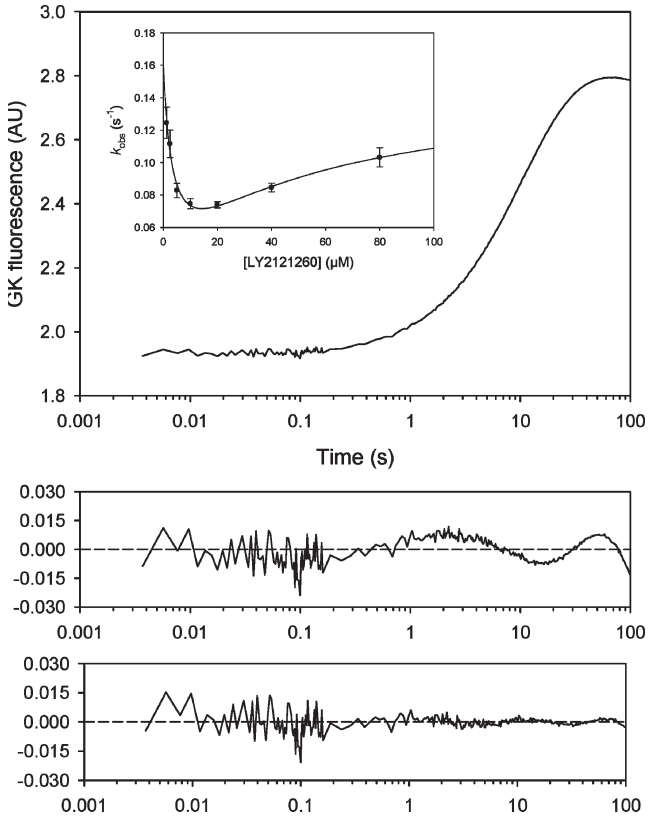

FIGURE 11: Kinetics of the interaction of LY2121260 with apo-GK in the absence of glucose. Apo-GK (1 μM) was rapidly mixed with LY2121260 (80 μM) in buffer A containing 5% DMSO, and the GK fluorescence was recorded (λ_{exc} = 295 nm). The upper frame shows the recorded transient; lower frames show the residuals for the best fit to one and two exponentials. The inset shows the dependence of k_{obs} against LY2121260 concentration. The solid line is a fit to eq 8 with parameters $k_{3\,LY}$ = 0.02 s^{-1}, $k_{-3\,LY}$ = 2.0 s^{-1}, $K_{D2\,LY}$ = 0.08 μM, $k_{2\,LY}$ = 0.15 s^{-1}, $k_{-2\,LY}$ = 0.03 s^{-1}, and $K_{D1\,LY}$ = 110 μM.

by $K_{D1\,CA}$. This hypothesis is supported by the similarity of the microscopic rate constants $k_{3\,Glc}/k_{-3\,Glc}$ and $k_{3\,CA}/k_{-3\,CA}$ determined from glucose or compound A binding to GK.

Results obtained for LY2121260 binding to GK were comparable to their compound A counterparts. Upon mixing of GK with LY2121260, in the absence of any ligand, GK fluorescence displayed a slow increase. The transient could be satisfactorily fitted with a double exponential (Figure 11). The slowest phase accounted for more than 80% of the signal amplitude. No fast quenching could be observed, maybe because of low amplitude. The slow increase of GK fluorescence was reminiscent of the transition induced by glucose and compound A. The observed rate constant for the major phase ($k_{obs\,LY}$) exhibited a biphasic dependence on LY2121260 concentration. $k_{obs\,LY}$ decreased hyperbolically from 0.12 s^{-1} at 2.5 μM LY2121260 to 0.07 s^{-1} between 10 and 20 μM LY2121260 before slowly increasing at concentrations above 20 μM and starting to level off at high LY2121260 concentrations (above 60 μM). This kinetic pattern is very similar to the one observed previously with glucose or compound A and suggests a similar kinetic mechanism based on the cyclic multiequilibrium between four species. Fitting of $k_{obs\,LY}$ to eq 6 led to high systematic errors on the parameter values. However, a good correlation was observed between the fit and the data (R_2 = 0.92) with the following parameters: $k_{3\,LY}$ = 0.02 s^{-1}, $k_{-3\,LY}$ = 2.0 s^{-1}, $K_{D2\,LY}$ = 0.08 μM, $k_{2\,LY}$ = 0.15 s^{-1}, $k_{-2\,LY}$ = 0.03 s^{-1}, and $K_{D1\,LY}$ = 110 μM (inset in Figure 11).

As observed with compound A, the equilibrium GK fluorescence intensity after binding with LY2121260 represented around 40% of the fluorescence intensity after LY2121260 binding to GK in the presence of glucose. Thus, in the absence of glucose, LY2121260 might not be able to fully shift the GK_{SO}−GK_O equilibrium toward GK_O.

Moreover, as observed with compound A, the kinetic $K_{D2\,LY}$ is similar to the equilibrium $K_{D\,LY}$ for GK_O. This broad similarity is in line with the suggestion that the preexisting equilibrium model describing apo-GK interaction with GKAs involves the same GK conformers than glucose binding, i.e., GK_{SO} and GK_O.

DISCUSSION.

It has long been recognized that GK plays a central role in glucose homeostasis as the primary glucose sensor in pancreatic β-cells and hepatocytes. The sensor properties of GK rely on its positive cooperativity toward its substrate glucose. Long before the resolution of GK crystal structures, this unusual kinetic behavior for a monomeric enzyme has been rationalized by the existence of a slow equilibrium between two distinct GK conformers, each one being able to bind glucose.

Interactions between GK and several GKAs have previously been studied by several techniques such as SPA, DSC, ITC, and steady-state kinetics (*17*). However, no microscopic rate constants for association and dissociation have been made available in the literature.

Preexisting Equilibrium and Glucose-Induced Conformational Changes: Unification of Apparently Conflicting Observations. Two independent fluorescence stopped-flow studies were recently published but resulted in two divergent glucose-binding mechanisms. On one hand, Heredia et al. (*13*) first described an apparently biphasic transient. A linear dependence of $k_{obs\,fast}$ on glucose concentration was observed, as well as a hyperbolic dependence of $k_{obs\,slow}$ on glucose concentration, consistent with a classical two-step "induced-fit" mechanism. Following this proposition, in the absence of glucose, apo-GK would be homogeneously present as the GK_{SO} conformer. Glucose would then slowly bind to GK_{SO} before inducing the isomerization to the GK_O conformer. On the other hand, Kim et al. (*14*) reported a monophasic transient, with a biphasic dependence of k_{obs} on glucose concentration. This biphasic dependence is the kinetic trademark of the cyclic four-step mechanism described by Schemes 2 and 3.

Repeating the same experiments in similar conditions, we observed up to four transitions. We suggest that both technical and analytical issues are responsible for those discrepancies. Concerning the fluorescence transients published by Heredia et al. (*13*), despite the low resolution of the figure, it seems clear that the residual plot displayed a fairly high systematic error, especially below 0.5 s. We suggest that addition of one or two exponential terms would improve the quality of the fit. By the same token, it is likely that extending the acquisition time up to 50−100 s would also help to uncover the slowest phase, as pointed out recently by Molnes et al. (*25*). Moreover, we did not observe a dependence of the fastest transition, k_{obs1}, against glucose concentration. This difference likely comes from the different fitting procedures used and suggests that the GK fluorescence is not directly sensitive to glucose binding. This suggestion is reinforced by the fact that the apparent second-order rate constant determined by Heredia et al. (*13*) (550 M^{-1} s^{-1}) is

orders of magnitude smaller than what could be expected for the binding of a small molecule to a protein (10^6-10^8 M^{-1} s^{-1}). Concerning the fluorescence transient published by Kim et al. (*14*), the combination of a fairly high instrumental noise with a single linear acquisition rate and a too short acquisition time might have masked the three additional low-amplitude transitions, leaving the major k_{obs3} as the only observable transition. Therefore, we are confident that GK does not obey the induced-fit mechanism proposed by Heredia et al. (*13*). Instead, the glucose dependence of the major transition we observed, k_{obs3}, is in agreement with the cyclic preexisting equilibrium model proposed by Kim et al. (*14*), as described by Scheme 2.

Nevertheless, questions remain regarding the three additional minor transitions observed in this work. Are those transitions representative of three steps of a global conformational change or only of subtle local rearrangements in the microenvironment of the three Trp present in GK, unrelated to the major conformational change from superopen to closed GK? Three pieces of evidence suggest that the three minority transitions actually reflect discrete steps of a global conformational change. First, those three phases are observed not only with GK intrinsic fluorescence but also with compound A fluorescence. As compound A signal is independent of Trp fluorescence, it is then clear that the observed transitions cannot only arise from slight structural relaxations in the local microenvironment of GK's Trp. Second, targeted molecular dynamics simulations (*27*) predicted that the overall conformational transition from closed to superopen GK might include three intermediates (P1, P2, and P3). Therefore, the complete transition from superopen to fully closed GK would also include five potentially observable conformers: $GK_{superopen}$, GK_{Int1}, GK_{Int2}, GK_{Int3}, and GK_{closed}, linked by four kinetic steps. Third, a fluorescence biphasic transient was observed after manually jumping apo-GK from 1 to 39 °C in the absence of glucose (*25*). Despite the low time resolution of the experiment that precluded the observations of fast transitions, it seems clear that additional conformational relaxations occurred during the dead time of the reported experiment. This result also supports the existence of multiple GK conformers preexisting in the absence of any ligand. In this context, extending the studies of Trp-mutated GKs (*25*, *26*) with pre-steady-state ligand binding experiments could shed more light on the nature of the fluorescence transients observed with wild-type GK. Moreover, detailed relaxation experiments such as T-jumps or pressure jumps might also help to characterize the complex conformational equilibria of wild-type GK.

Preexisting Equilibrium and GK Activator Binding. Previous ITC-based studies reported the absence of GKA binding to GK in the absence of glucose (*18*). In contrast, our fluorescence equilibrium titration experiment unambiguously showed that at least compound A can actually bind to GK in the absence of glucose. Differences in experimental conditions between ITC and fluorescence titrations combined to calorimetric contributions from the conformational changes accompanying GKA binding to apo-GK might have hidden GKA binding when monitored by ITC.

Based on the results from the glucose binding study, the simplified preexisting equilibrium model states that, in the absence of glucose, GK slowly shuttles between two conformations. Throughout this paper, these conformations were assigned to the superopen and open conformations, following Kamata et al. (*12*). Although reasonable, there is currently no experimental evidence confirming the validity of this assumption in solution. Based on this simplified kinetic model and on the structural observation that the allosteric site is not formed on GK_{SO}, GKAs are theoretically restricted to bind the minority GK_O present in the absence of glucose and consequently to shift the $GK_{SO}-GK_O$ equilibrium toward GK_O. Kinetically, this situation is equivalent to route A and results in a decrease of the k_{obs} associated with the $GK_{SO}-GK_O$ transition with increasing GKA concentration, as measured via GK fluorescence. Experimentally, a decrease of k_{obs} is observed for the lowest GKA concentrations used, governed by the microscopic rate constants $k_{3\,GKA}$ and $k_{-3\,GKA}$, in reasonable agreement with their counterparts determined from the glucose binding data. Unexpectedly, a slight increase of k_{obs} for higher GKA concentrations is also measured. This increase can be explained by an operational route B, with GK_{SO} being also able to bind GKA, although with a modest K_D (around 50−100 μM). This kinetic observation reinforces the equilibrium binding data and clearly establishes that GK binds GKA even in the absence of glucose. Furthermore, it strongly suggests that the conformer referred to so far as GK_{SO} does not correspond to the superopen conformation crystallographically described, as it is able to bind GKA. It could then reasonably be assigned to one of the three intermediate conformers poised between the superopen and open structure, predicted by the molecular dynamics results (*27*). A tempting hypothesis would be to assign GK_{SO} to GK_{Int1} and GK_O to GK_{Int2} (P3 and P2 states, respectively (*27*)). Indeed, the free energy landscape derived from the targeted molecular dynamics suggests that the greatest energy barrier lies between $GK_{superopen}$ and GK_{Int1}, followed by the GK_{Int1} to GK_{Int2} barrier, the GK_{Int2} to GK_{Int3} barrier, and finally the GK_{Int3} to GK_{closed} barrier. Such a situation would kinetically translate in the following relationship: $k_{superopen\,to\,Int1} < k_{Int1\,to\,Int2} < k_{Int2\,to\,Int3} < k_{Int3\,to\,closed}$, suggesting that $k_{superopen\,to\,Int1} = k_{obs4}$, $k_{Int1\,to\,Int2} = k_{obs3}$, $k_{Int2\,to\,Int3} = k_{obs2}$, and $k_{Int3\,to\,closed} = k_{obs1}$.

Additionally, compared to the kinetic parameters determined from the simplified glucose binding model, the 10-fold difference between $k_{2\,GKA}$ and $k_{2\,Glc}$ suggests that bound GKA perturbs the conformational equilibrium by slowing the transition from GK_{SO} to GK_O, likely because of steric hindrance.

As a conclusion, the cyclic preexisting equilibrium model described by Schemes 2 and 3 should be regarded as a simplified mechanism that might explain the main kinetic features of GK interactions with glucose and GKAs. However, taken as a whole, our data strongly suggest that this simplified pathway does not account for minority kinetic transitions that likely reflect discrete steps in the multiple GK conformational equilibria. Although more work is clearly needed, we propose that instead of shuttling between two relatively open conformations in the absence of glucose, GK might be able to perform an extensive sampling of the accessible conformational space delimited by the superopen and the fully closed limiting conformations and driven by the likely existence of three stable intermediate conformers. Following this interpretation and the additional elements developed in the next paragraph, we propose a working kinetic model depicted by Scheme 5.

An important question still remains unresolved: are the superopen and fully closed conformations able to bind glucose? Indeed, superopen GK does not display a fully structured glucose binding site, and fully closed GK may restrict glucose accessibility to the active site. On one hand, the lack of glucose dependence for the three low-amplitude transitions apparently suggests that the GK conformers giving rise to those additional transients do not bind

Scheme 5: Qualitative Working Model Describing the GK Conformational Dynamics and Interactions with Its Ligands[a]

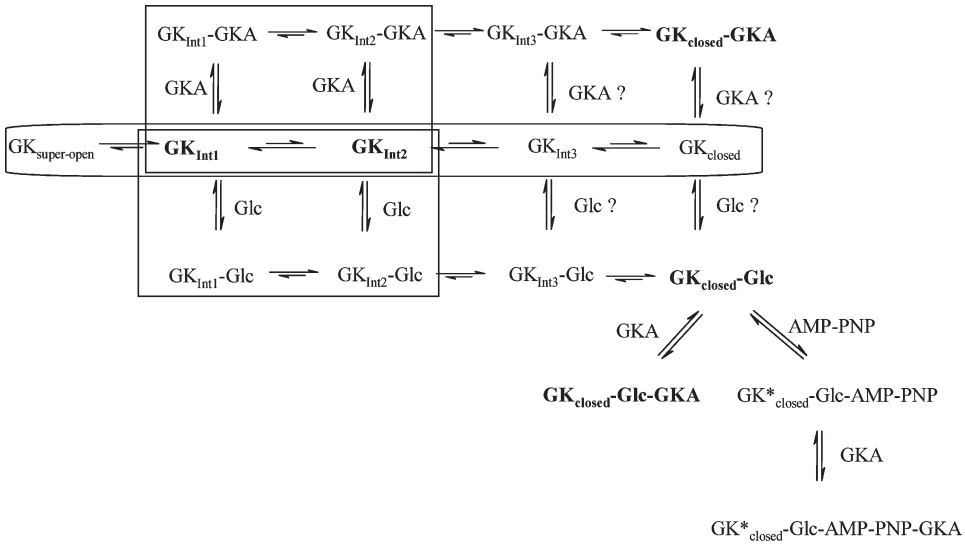

[a] The rounded rectangle qualitatively describes the putative conformational dynamics of apo-GK in the absence of ligands. $GK_{superopen}$ and GK_{closed} refer to the two crystallographic structures from Kamata et al. (*12*). GK_{Int1}, GK_{Int2}, and GK_{Int3} are three intermediate conformers. GK_{Int1} and GK_{Int2} are the two major conformers, GK_{Int1} being the most favored conformer. GKA binding to apo-GK is described above the apo-GK rectangle, leading to the major GK_{closed}−GKA complex. Glucose binding to apo-GK is described by the first line below the apo-GK rectangle, leading to the major GK_{closed}−Glc complex. Steps labeled with an interrogation mark have not been characterized in this study. The two rectangular boxes are identical to Scheme 3 and Scheme 2. GKA binding to the preformed binary GK_{closed}−Glc complex and ternary GK_{closed}−Glc−AMP-PNP complex is described in the lower part of the mechanism.

glucose, at least in the investigated glucose concentrations where reliable rate constants could be measured. On the other hand, very weak glucose binding to the superopen GK and strong glucose binding to closed GK conformers cannot be ruled out by our data. Moreover, similar $K_{D\,Glc}$ for two different GK conformers would presumably also hide any glucose dependence of the associated observed rate constant. In this regard, advanced molecular dynamics and docking studies between GK and glucose and GKAs could be informative.

Evaluation of Pre-Steady-State Kinetics as a Tool for Ranking GK Activators. GKAs binding to closed GK revealed a k_{on} rate too slow (1×10^6 M^{-1} s^{-1}) to be diffusion-limited, suggesting a relatively occluded access to the allosteric site. The k_{on} for compound A and LY212160 were broadly similar, with a slightly faster k_{on} for the smaller compound A. This subtle difference might come from a sterically easier access to the allosteric site for the somewhat smaller compound A. The k_{off} were slow and very close for the two GKAs studied. Interestingly, the k_{off} were in the same range than some steps of the GK conformational changes. This similarity might suggest that the rate-limiting step for dissociation of the GKAs is linked to a conformational change. Therefore, it seems that difference in k_{on} and not in k_{off} is the main factor governing K_D difference between GKAs. Testing the binding of smaller and bulkier GKAs should allow validation of this hypothesis.

Although the potential correlation between GKA binding parameters and GK activation strength has not been studied yet, pre-steady-state fluorescence kinetics represents a useful tool to precisely characterize GKAs binding to closed GK conformers and to rank those small molecules according to their k_{on}, k_{off}, and/or K_D.

Kinetic Suggestion for a Previously Unobserved Superclosed Conformation after AMP-PNP Binding? A previous fluorescence study suggested that addition of the nonhydrolyzable ATP analogue AMP-PNP to closed GK led to a quenching of GK intrinsic fluorescence, allowing the determination of its intrinsic K_D (*14*). Molnes et al. (*25*) suggested that this observation might have been biased by the absence of corrections for the nucleotide absorbance and the resulting inner filtering. Using *N*-acetyltryptophanamide as a control, we confirmed that the nucleotide inner-filter effect is responsible for the apparent GK fluorescence quenching reported previously (data not shown). Therefore, no K_D could be accurately derived from the data.

Using the fluorescence stopped-flow approach with a short path length cell minimizing inner filtering, mixing AMP-PNP with GK led to a slow, barely visible quenching of GK fluorescence, with or without glucose preequilibration (data not shown). No linear increase of k_{obs} with the AMP-PNP concentration was observed; thus the transients do not reflect the bimolecular binding of AMP-PNP and GK. No clear variation of k_{obs} with increasing AMP-PNP concentration could be observed. Those results are in qualitative agreement with previous observations (*14*). It could be concluded that GK fluorescence is not directly sensitive to AMP-PNP binding and that it does not provide any information related to AMP-PNP binding.

However, when AMP-PNP was allowed to equilibrate with GK and glucose before addition of GKAs, a small but significant increase of $k_{on\,GKA}$ and $k_{off\,GKA}$ was observed, with a more pronounced effect for compound A than LY2121260. Although $K_{D\,GKA}$ was not modified by the addition of AMP-PNP because the increased k_{on} was compensated by the increased k_{off}, this perturbation of the binding rate constants suggests that binding of AMP-PNP induced a conformational change. Because compound A was more sensitive than LY2121260 to the AMP-PNP-induced conformational alteration, it is unlikely that binding of AMP-PNP induced a global conformational change to a "superclosed" conformer. Instead, AMP-PNP binding may locally influence the structure or dynamics of the allosteric site, rendering it a little more accessible to compound A but not to the bulkier LY2121260.

Preexisting Equilibrium and Implications for the Allosteric Regulation of GK. Postexpression regulation of GK activity is of crucial importance for the physiology of hepatocytes and pancreatic β-cells. In the liver, control of the GK activity is provided by the GK regulatory protein (GKRP) that binds to GK and inhibits the enzyme when low glucose conditions prevail (*28*, *29*). Inhibition is also mediated by small molecules such as palmitoyl-CoA (*30*, *31*). Recently, interaction and activation of GK by the bifunctional enzyme 6-phosphofructo-2-kinase/fructose-2,6-biphosphatase (PFK/FBP) has been reported (*32*, *33*). Besides this potential physiological activator, GK is strongly activated by synthetic GKAs.

Presumably, the key of the regulation of the GK activity is the stabilization of a specific GK conformation via binding of effectors to this GK conformer. Schematically, activators will specifically bind active GK conformers, i.e., closed conformations, whereas inhibitors will specifically bind inactive GK conformers, i.e., open conformations. Binding of an effector to a specific GK conformer will pull the complex out of the GK conformational equilibrium and force the system to reequilibrate, resulting in a net increase of the total concentration of the targeted conformer. Thus, known GK effectors can essentially be seen as reversible conformational traps.

In this context, the preequilibrium model states that whatever the glucose concentration considered, yet in the physiological range, GK will still be able to populate unfavored minority conformational states. In other words, while high glucose concentration favors closed GK conformers, it does not eliminate open conformers. Similarly, low glucose concentration favors the open conformers, but closed conformers are still present. These minor conformational states provide essential anchoring points for effectors to finely tune GK conformational landscape, in turn responsible for the GK activity. This model qualitatively accounts for the influence of glucose and GKAs on the GK−GKRP interaction. Indeed, in low glucose concentration, open GK conformers will prevail and bind to GKRP. However, a low amount of closed GK conformers will still be present and available to bind glucose or GKAs. Addition of glucose and/or GKAs will shift the equilibrium toward the closed conformers and induce the dissociation of the GK−GKRP complex. Thus, every molecule able to stabilize the closed GK conformers, potentially including PFK−FBP, is expected to impair the GK−GKRP interaction. The k_{on} and k_{off} rate constants determining the strength of the interaction between GK and the effector will modulate its effect on the GK−GKRP complex. Quantitative predictions of the effect of modulators will require the estimation of the complete set of rate constants governing the model. The recent molecular characterization of the GK−GKRP interaction (*18*) is a valuable step in this perspective.

Discovery of a GKA specific for the pancreatic GK isoform could be a desired outcome. However, in light of our model and from a strictly molecular point of view, the search for a potent GKA that would strictly exert its activity on the pancreatic GK isoform is presumably vain, as such a molecule would also likely have a significant effect on the GK−GKRP interaction on the liver.

ACKNOWLEDGMENT

We are grateful to Dr. S. Goldstein, Dr. M. Wierzbicki, and their teams for the GKA synthesis, to Pr. G. Branlant and his team for granting us access to an Applied PhotoPhysics stopped-flow instrument, and to Dr. A. Van Dorsselear, Dr. S. Sanglier-Cianferani, and C. Atmanene for MS determination.

REFERENCES

1. Matschinsky, F. M. (1990) Glucokinase as glucose sensor and metabolic signal generator in pancreatic beta-cells and hepatocytes. *Diabetes39*, 647–652.
2. Agius, L., Peak, M., Newgard, C. B., Gomez-Foix, A. M., and Guinovart, J. J. (1996) Evidence for a role of glucose-induced translocation of glucokinase in the control of hepatic glycogen synthesis. *J. Biol. Chem.271*, 30479–30486.
3. Vionnet, N., Stoffel, M., Takeda, J., Yasuda, K., Bell, G. I., Zouali, H., Lesage, S., Velho, G., Iris, F., Passa, P., Froguel, P., and Cohen, D. (1992) Nonsense mutation in the glucokinase gene causes early-onset non-insulin-dependent diabetes mellitus. *Nature356*, 721–722.
4. Matschinsky, F., Liang, Y., Kesavan, P., Wang, L., Froguel, P., Velho, G., Cohen, D., Permutt, M. A., Tanizawa, Y., and Jetton, T. L. (1993) Glucokinase as pancreatic beta cell glucose sensor and diabetes gene. *J. Clin. Invest.92*, 2092–2098.
5. Christesen, H. B., Jacobsen, B. B., Odili, S., Buettger, C., Cuesta-Munoz, A., Hansen, T., Brusgaard, K., Massa, O., Magnuson, M. A., Shiota, C., Matschinsky, F. M., and Barbetti, F. (2002) The second activating glucokinase mutation (A456 V): implications for glucose homeostasis and diabetes therapy. *Diabetes51*, 1240–1246.
6. Cuesta-Munoz, A. L., Huopio, H., Otonkoski, T., Gomez-Zumaquero, J. M., Nanto-Salonen, K., Rahier, J., Lopez-Enriquez, S., Garcia-Gimeno, M. A., Sanz, P., Soriguer, F. C., and Laakso, M. (2004) Severe persistent hyperinsulinemic hypoglycemia due to a de novo glucokinase mutation. *Diabetes53*, 2164–2168.
7. Storer, A. C., and Cornish-Bowden, A. (1977) Kinetic evidence for a "mnemonical" mechanism for rat liver glucokinase. *Biochem. J.165*, 61–69.
8. Neet, K. E., and Ainslie, G. R.Jr. (1980) Hysteretic enzymes. *Methods Enzymol.64*, 192–226.
9. Cornish-Bowden, A., and Cardenias, A. (2004) in *Glucokinase and Glycemic Disease: from Basics to Novel Therapeutics* (Matschinsky, F., and Magnuson, M. A., Eds.) pp 125−134, Karger, Basel, Switzerland.
10. Neet, K. E., Keenan, R. P., and Tippett, P. S. (1990) Observation of a kinetic slow transition in monomeric glucokinase. *Biochemistry29*, 770–777.
11. Lin, S. X., and Neet, K. E. (1990) Demonstration of a slow conformational change in liver glucokinase by fluorescence spectroscopy. *J. Biol. Chem.265*, 9670–9675.
12. Kamata, K., Mitsuya, M., Nishimura, T., Eiki, J., and Nagata, Y. (2004) Structural basis for allosteric regulation of the monomeric allosteric enzyme human glucokinase. *Structure12*, 429–438.
13. Heredia, V. V., Thomson, J., Nettleton, D., and Sun, S. (2006) Glucose-induced conformational changes in glucokinase mediate allosteric regulation: transient kinetic analysis. *Biochemistry45*, 7553–7562.
14. Kim, Y. B., Kalinowski, S. S., and Marcinkeviciene, J. (2007) A pre-steady state analysis of ligand binding to human glucokinase: evidence for a preexisting equilibrium. *Biochemistry46*, 1423–1431.
15. Sarabu, R., and Grimsby, J. (2005) Targeting glucokinase activation for the treatment of type 2 diabetes—a status review. *Curr. Opin. Drug Discovery Dev.8*, 631–637.
16. Grimsby, J., Sarabu, R., Corbett, W. L., Haynes, N. E., Bizzarro, F. T., Coffey, J. W., Guertin, K. R., Hilliard, D. W., Kester, R. F., Mahaney, P. E., Marcus, L., Qi, L., Spence, C. L., Tengi, J., Magnuson, M. A., Chu, C. A., Dvorozniak, M. T., Matschinsky, F. M., and Grippo, J. F. (2003) Allosteric activators of glucokinase: potential role in diabetes therapy. *Science301*, 370–373.
17. Ralph, E. C., Thomson, J., Almaden, J., and Sun, S. (2008) Glucose modulation of glucokinase activation by small molecules. *Biochemistry47*, 5028–5036.
18. Anderka, O., Boyken, J., Aschenbach, U., Batzer, A., Boscheinen, O., and Schmoll, D. (2008) Biophysical characterization of the interaction between hepatic glucokinase and its regulatory protein: impact of physiological and pharmacological effectors. *J. Biol. Chem.283*, 31333–31340.
19. Efanov, A. M., Barrett, D. G., Brenner, M. B., Briggs, S. L., Delaunois, A., Durbin, J. D., Giese, U., Guo, H., Radloff, M., Gil, G. S., Sewing, S., Wang, Y., Weichert, A., Zaliani, A., and Gromada, J. (2005) A novel glucokinase activator modulates pancreatic islet and hepatocyte function. *Endocrinology146*, 3696–3701.
20. Brocklehurst, K. J., Payne, V. A., Davies, R. A., Carroll, D., Vertigan, H. L., Wightman, H. J., Aiston, S., Waddell, I. D., Leighton, B., Coghlan, M. P., and Agius, L. (2004) Stimulation of hepatocyte glucose metabolism by novel small molecule glucokinase activators. *Diabetes53*, 535–541.

21. Castelhano, A. L., Dong, H., Fyfe, M. C., Gardner, L. S., Kamikozawa, Y., Kurabayashi, S., Nawano, M., Ohashi, R., Procter, M. J., Qiu, L., Rasamison, C. M., Schofield, K. L., Shah, V. K., Ueta, K., Williams, G. M., Witter, D., and Yasuda, K. (2005) Glucokinase-activating ureas. *Bioorg. Med. Chem. Lett.15*, 1501–1504.
22. Heuser, S., Barrett, D. G., Berg, M., Bonnier, B., Kahl, A., De La Puente, M. L., Oram, N., Riedl, R., Roettig, U., Sanz Gil, G., Seger, E., Steggles, D. J., Wanner, J., and Weichert, A. G. (2006) Synthesis of novel cyclopropylic sulfones and sulfonamides acting as glucokinase activators. *Tetrahedron Lett.47*, 2675–2678.
23. Storer, A. C., and Cornish-Bowden, A. (1974) The kinetics of coupled enzyme reactions. Applications to the assay of glucokinase, with glucose 6-phosphate dehydrogenase as coupling enzyme. *Biochem. J.141*, 205–209.
24. Roehrl, M. H., Wang, J. Y., and Wagner, G. (2004) A general framework for development and data analysis of competitive high-throughput screens for small-molecule inhibitors of protein-protein interactions by fluorescence polarization. *Biochemistry43*, 16056–16066.
25. Molnes, J., Bjorkhaug, L., Sovik, O., Njolstad, P. R., and Flatmark, T. (2008) Catalytic activation of human glucokinase by substrate binding: residue contacts involved in the binding of D-glucose to the super-open form and conformational transitions. *FEBS J.275*, 2467–2481.
26. Zelent, B., Odili, S., Buettger, C., Shiota, C., Grimsby, J., Taub, R., Magnuson, M. A., Vanderkooi, J. M., and Matschinsky, F. M. (2008) Sugar binding to recombinant wild-type and mutant glucokinase monitored by kinetic measurement and tryptophan fluorescence. *Biochem. J.413*, 269–280.
27. Zhang, J., Li, C., Chen, K., Zhu, W., Shen, X., and Jiang, H. (2006) Conformational transition pathway in the allosteric process of human glucokinase. *Proc. Natl. Acad. Sci. U.S.A.103*, 13368–13373.
28. Van Schaftingen, E. (1989) A protein from rat liver confers to glucokinase the property of being antagonistically regulated by fructose 6-phosphate and fructose 1-phosphate. *Eur. J. Biochem.179*, 179–184.
29. Vandercammen, A., and Van Schaftingen, E. (1990) The mechanism by which rat liver glucokinase is inhibited by the regulatory protein. *Eur. J. Biochem.191*, 483–489.
30. Tippett, P. S., and Neet, K. E. (1982) Specific inhibition of glucokinase by long chain acyl coenzymes A below the critical micelle concentration. *J. Biol. Chem.257*, 12839–12845.
31. Tippett, P. S., and Neet, K. E. (1982) An allosteric model for the inhibition of glucokinase by long chain acyl coenzyme A. *J. Biol. Chem.257*, 12846–12852.
32. Baltrusch, S., Lenzen, S., Okar, D. A., Lange, A. J., and Tiedge, M. (2001) Characterization of glucokinase-binding protein epitopes by a phage-displayed peptide library. Identification of 6-phosphofructo-2-kinase/fructose-2,6-bisphosphatase as a novel interaction partner. *J. Biol. Chem.276*, 43915–43923.
33. Smith, W. E., Langer, S., Wu, C., Baltrusch, S., and Okar, D. A. (2007) Molecular coordination of hepatic glucose metabolism by the 6-phosphofructo-2-kinase/fructose-2,6- bisphosphatase:glucokinase complex. *Mol. Endocrinol.21*, 1478–1487.